CORRECTION POSTED 30 OCTOBER 2023

ALLERGY

Laboratory mice with a wild microbiota generate strong allergic immune responses

Junjie Ma[1]†, Egon Urgard[1,2]†, Solveig Runge[3,4], Cajsa H. Classon[1], Laura Mathä[1], Julian M. Stark[1], Liqin Cheng[1], Javiera A. Álvarez[1], Silvia von Zedtwitz[5], Austeja Baleviciute[1], Sergio Martinez Hoyer[1], Muzhen Li[1], Anne Marleen Gernand[5], Lisa Osbelt[6], Agata Anna Bielecka[6], Till R. Lesker[6], Huey-Jy Huang[7], Susanne Vrtala[7], Louis Boon[8], Rudi Beyaert[9,10], Mikael Adner[11], Itziar Martinez Gonzalez[1], Till Strowig[6,12], Juan Du[1], Susanne Nylén[1]*‡, Stephan P. Rosshart[3,5]*‡, Jonathan M. Coquet[1,2]*‡

Allergic disorders are caused by a combination of hereditary and environmental factors. The hygiene hypothesis postulates that early-life microbial exposures impede the development of subsequent allergic disease. Recently developed "wildling" mice are genetically identical to standard laboratory specific pathogen–free (SPF) mice but are housed under seminatural conditions and have rich microbial exposures from birth. Thus, by comparing conventional SPF mice with wildlings, we can uncouple the impact of lifelong microbial exposures from genetic factors on the allergic immune response. We found that wildlings developed larger populations of antigen-experienced T cells than conventional SPF mice, which included interleukin-10–producing CD4 T cells specific for commensal *Lactobacilli* strains and allergy-promoting T helper 2 (T_H2) cells. In models of airway exposure to house dust mite (HDM), recombinant interleukin-33, or *Alternaria alternata*, wildlings developed strong allergic inflammation, characterized by eosinophil recruitment, goblet cell metaplasia, and antigen-specific immunoglobulin G1 (IgG1) and IgE responses. Wildlings developed robust de novo T_H2 cell responses to incoming allergens, whereas preexisting T_H2 cells could also be recruited into the allergic immune response in a cytokine-driven and TCR-independent fashion. Thus, wildling mice, which experience diverse and lifelong microbial exposures, were not protected from developing pathological allergic immune responses. Instead, wildlings mounted robust allergic responses to incoming allergens, shedding new light on the hygiene hypothesis.

INTRODUCTION

The incidence of allergies has risen at an alarming rate over the past century. In some developed countries, approximately 30% of children are affected by rhinitis, atopic dermatitis, or asthma by the age of 5 years (*1*). Genetic factors play an important role in susceptibility to allergic disease because children born to allergic parents are several times more likely to suffer from allergy, whereas concordance between monozygotic twins is approximately 50% (*2*). Genome-wide association studies have pinpointed several loci involved in the development of allergy (*2*), including human leukocyte antigen D alleles, which encode for major histocompatibility class II (MHC-II) molecules that are important for the activation of CD4 T cells.

However, the notable rise in allergic disorders during the 20th century cannot solely be explained by genetic factors. Altered exposure to microbes, owing to improved sanitation, vaccination, widespread use of antibiotics, and a changing diet, are repeatedly proposed as the major factors driving the rapid rise in allergic disease incidence (*3*). Studies have linked a lower incidence of allergic disease to high microbial diversity in the intestine and greater microbial exposures in rural settings, for instance, from animal barns or by drinking raw milk (*4*–*9*). However, microbial exposures are not always linked to reduced allergic disease, and it is evident that some pulmonary infections may potentiate the development of asthma in children (*10*–*14*).

Laboratory mice are advantageous to study allergy because their genetics and environment can be closely controlled. In studies that analyzed the influence of microbes on allergic disease, germ-free (GF) mice were found to have higher levels of circulating immunoglobulin E (IgE) antibodies, developed more severe anaphylactic responses to ingested antigens, and had more vigorous inflammatory responses to inhaled antigens, in comparison with standard laboratory specific pathogen–free (SPF) mice (*15*–*17*). This implied that the intestinal microbiota of SPF mice contained microbes that regulated the development of allergic immune responses to ingested antigens.

However, SPF mice themselves have been increasingly sanitized by vendors and institutional animal facilities around the world and

[1]Department of Microbiology, Tumor and Cell Biology (MTC), Karolinska Institutet, Stockholm, Sweden. [2]Leo Foundation Skin Immunology Research Centre, Department of Immunology and Microbiology, University of Copenhagen, Denmark. [3]Department of Microbiome Research, University Hospital Erlangen, Friedrich-Alexander-Universität Erlangen-Nürnberg (FAU), Erlangen, Germany. [4]Faculty of Biology, University of Freiburg, Freiburg, Germany. [5]Department of Medicine II, Medical Center–University of Freiburg, Faculty of Medicine, Freiburg, Germany. [6]Department of Microbial Immune Regulation, Helmholtz Center for Infection Research, Braunschweig, Germany. [7]Division of Immunopathology, Department of Pathophysiology and Allergy Research, Center for Pathophysiology, Infectiology, and Immunology, Medical University of Vienna, Vienna, Austria. [8]JJP Biologics, Warsaw, Poland. [9]VIB Centre for Inflammation Research, Ghent, Belgium. [10]Department of Biomedical Molecular Biology, Ghent University, Ghent, Belgium. [11]Institute of Environmental Medicine and Centre for Allergy Research, Karolinska Institutet, Stockholm, Sweden. [12]Center for Individualized Infection Medicine (CiiM), a joint venture between the Helmholtz-Centre for Infection Research (HZI) and the Hannover Medical School (MHH), Hannover, Germany.
*Corresponding author. Email: jonathan.coquet@ki.se (J.M.C.); stephan.rosshart@uk-erlangen.de (S.P.R.); susanne.nylen@ki.se (S.N.)
†These authors contributed equally to this work.
‡These authors contributed equally to this work.

have been criticized for their lack of microbial diversity (*18*). Several recent studies show that mice housed under SPF conditions fail to faithfully replicate the immune responses of free-living humans (*19*–*23*). In studies of wild mice, pet store mice, or SPF mice made wild by fecal material transfer or co-housing, researchers noted that these animals mounted more effective immune responses to influenza, bacteria, tumors, and parasites than conventional laboratory SPF mice and better reflected the human situation (*19*, *21*, *22*).

Because direct comparisons between conventional laboratory mice and wild mice are complicated by genetic disparities, Rosshart and colleagues (*21*) recently described a system for the transfer of common C57BL/6 mouse embryos into wild mouse surrogate mothers, generating so-called wildling mice. Wildling mice were found to acquire a fulminant gut, skin, and vaginal microbiota, a representative breadth of naturally occurring pathogens, and many of the broader immune features of wild mice. Thus, comparing the development of allergic inflammation in wildlings versus conventional SPF mice provides an opportunity to test whether the rich microbial composition of wildlings exerts a regulatory effect on allergic immune responses. In this study, we expose C57BL/6 SPF mice and C57BL/6 wildlings to allergens and alarmins and characterize the influence of early life and continuous microbial exposures on allergic immune responses.

RESULTS

The housing conditions of wildling mice ensure lifelong exposures to diverse microbial communities

It is known that wildlings are stably colonized with a natural wild mouse microbiota at all immunological barrier sites for at least five generations and maintain stable phenotypes under conventional SPF housing conditions (*21*). However, humans are subject to early life and continuous microbial exposure, both of which play a role in allergic diseases. To better acknowledge these real-life conditions and to more closely mimic human microbial exposures that may affect allergic outcomes, we have tailored the wildling model to specifically match the needs of this study. To accomplish this, we created seminatural housing conditions through cage supplementation with natural materials such as hay, compost, and fomites from actual wild mice (Fig. 1A). In addition, litters from different breeding pairs were fraternized in large cages to increase their microbial exposures in adolescence. The specific hygiene standards of wildlings and the conventional SPF mice used for this study can be found in table S1. 16*S* ribosomal RNA (rRNA) sequencing of feces confirmed large differences in the microbiota composition of adult SPF mice and wildlings (Fig. 1B). Moreover, analysis of cecal contents and fecal matter found substantial amounts of fungi in the gastrointestinal tracts of wildlings but virtually no fungi in conventional laboratory SPF mice (fig. S1). Further analysis of the fungal community structure showed considerable variability in fungal composition between wildlings with some mice primarily colonized by fungi of the Saccharomycetaceae family and others showing a more diverse pattern of colonization (fig. S1).

Antigen-experienced T cells are expanded in wildling mice after weaning

We characterized the immune cell composition of conventional SPF mice and wildlings at days 5, 14, 28, and 98 after birth. Thymic cellularity was comparable between SPF mice and wildlings at most time points except at day 28, where wildling mice had significantly fewer thymocytes (Fig. 1, C and D). At all time points, the frequency of $CD4^+CD8^+$ [double-positive (DP)], CD4 single-positive (SP) ($CD4^+CD8^-$), CD8 SP ($CD8^+CD4^-$), and $CD4^-CD8^-$ [double-negative (DN)] thymocytes was comparable between SPF mice and wildlings (Fig. 1, C and D). Progenitor subsets within DN thymocytes were also comparable across all time points (fig. S2, A and B).

Wildlings and SPF mice had comparable numbers of mature T cells in the spleen at days 5, 14, and 28 postnatal, but the T cell compartment in wildlings expanded significantly more thereafter (Fig. 1, E and F). Antigen-experienced $CD44^+$ effector CD4 ($Foxp3^-$) and CD8 T cells were comparable in frequency and number until day 28. At day 98, a notable increase in $CD44^+$ CD4 and CD8 T cells was observed in wildlings compared with SPF mice (Fig. 1F). The expansion in antigen-experienced CD8 T cells was associated with increases into both "true memory" CD8 (CD8 T_{TM}) and "virtual memory" CD8 T (CD8 T_{VM}) (*24*) cell subsets in the spleen (Fig. 1F and fig. S2C). Deviations in frequencies of naïve CD8 T, CD8 T_{TM}, and CD8 T_{VM} cell subsets were already evident at day 14 in wildlings (fig. S2C), even if absolute cell numbers were not altered at this time. Analysis of CD44 and CD62L expression revealed expanded populations of both central and effector memory CD8 T cells in adult wildling spleen (fig. S2D). Splenic $Foxp3^+$ suppressive regulatory T (T_{reg}) cells were numerically reduced in wildlings at day 28 but present at higher numbers in wildlings at day 98 (Fig. 1F). In line with heightened levels of antigen-experienced T cells, circulating IgG1, IgG2c, IgA, and IgE were all markedly higher in adult wildlings compared with SPF mice (fig. S2E), and a small increase in IgM was also observed.

Wildlings produce IL-10 in an MHC-II–dependent manner in response to various commensals and pathogens

Next-generation sequencing of the gut microbiome has suggested that humans are colonized by putative "good" or "bad" bacteria that may regulate or exacerbate inflammatory processes in the gut and at distal sites (*25*). For instance, strains of *Lactobacilli* have been repeatedly linked to inducing suppressive immune responses that could reduce allergy in the first years of life (*26*). To analyze the wildling response to certain commensals and putative pathogens, we cultured splenocytes with a panel of heat-killed microbes in the presence or absence of MHC-II–blocking antibody and analyzed the culture supernatants for interferon-γ (IFN-γ), interleukin-4 (IL-4), IL-5, IL-13, IL-17, and IL-10. SPF mice and wildlings readily produced IFN-γ in response to culture with *Staphylococcus aureus*, *Salmonella typhimurium*, *Escherichia coli*, and *Klebsiella pneumoniae* that was largely abrogated when MHC-II was blocked (Fig. 1G and table S2 for absolute quantities). *S. aureus* induced some IL-13 production from wildlings preferentially (Fig. 1G), whereas IL-17 was detected only sporadically in lymphocyte cultures. The immunoregulatory cytokine IL-10 was more highly produced in splenocyte cultures from wildlings in response to microbes including commensals *Lactobacillus reuteri* and *Lactobacillus johnsonii* and the putative pathogen *S. aureus* (Fig. 1G and table S2). IL-10 production was also largely impaired by MHC-II blockade, suggesting that CD4 T cells were the main source of this cytokine. Thus, wildling mice are marked by an expansion of

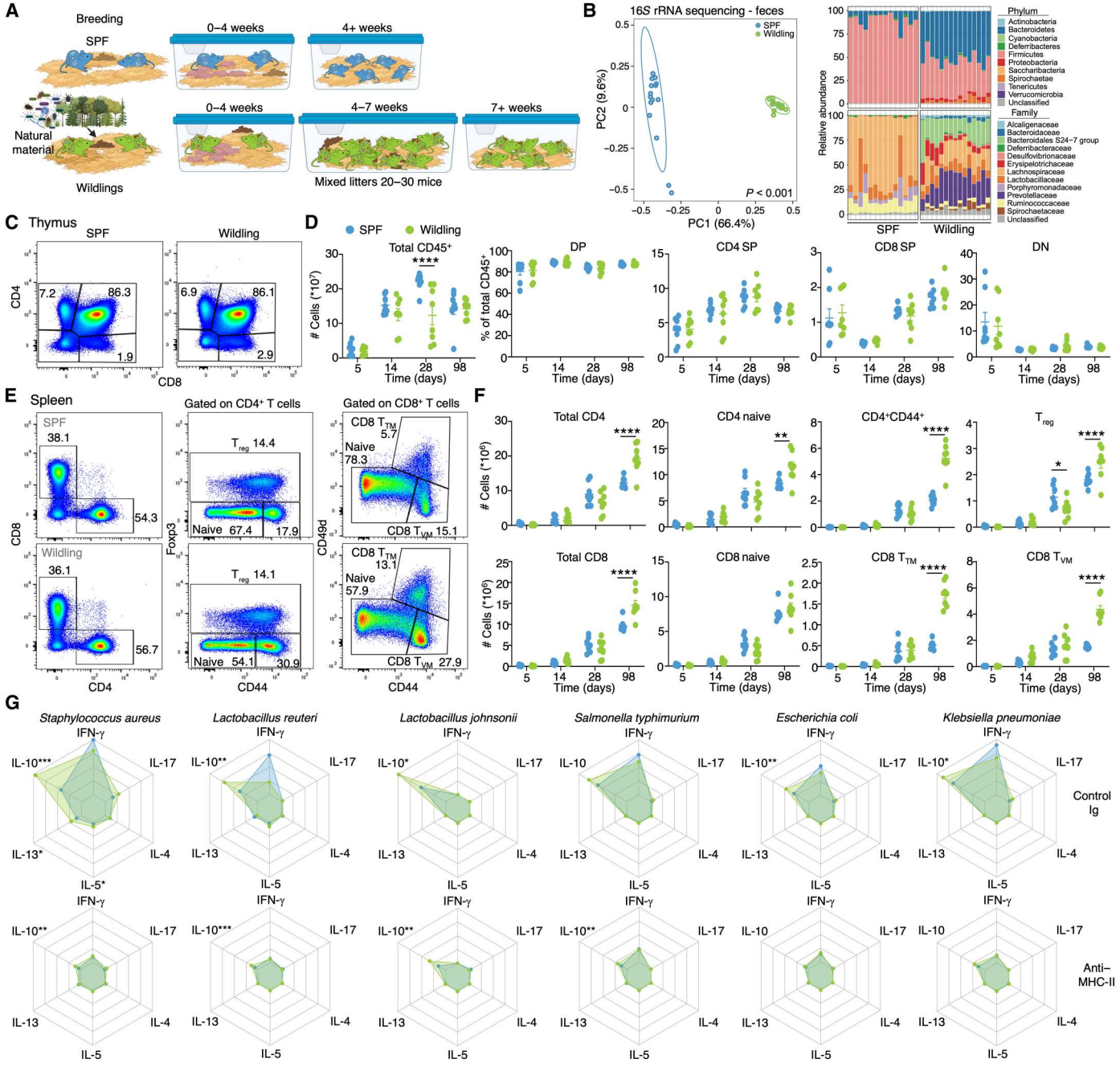

Fig. 1. Wildlings contain large populations of antigen-experienced T cells that produce IL-10 in response to commensals. (**A**) Clean housing conditions of SPF and seminatural conditions of wildling mice. (**B**) The gastrointestinal bacterial microbiome of B6 wildlings and conventional laboratory SPF mice was profiled by 16*S* rRNA sequencing. Left: Unweighted UniFrac PCoA. Right: Relative abundance at the rank of phylum and family. Data shown are from 14 or 15 independent biological replicates per group, and significance was determined by permutational multivariate ANOVA. (**C**) Representative flow plots of CD4 versus CD8 expression in thymi of SPF and wildling mice. Numbers indicate frequency of cells in the indicated gate. (**D**) Graphs depict total CD45$^+$ cells and numbers of CD4$^+$CD8$^+$ (DP), CD4$^+$CD8$^-$ (CD4 SP), CD4$^-$CD8$^+$ (CD8 SP), and CD4$^-$CD8$^-$ (DN) cells in the thymi of SPF and wildling mice at days 5, 14, 28, and 98 after birth. (**E**) Representative flow plots of CD8 versus CD4 expression on gated CD3$^+$ cells (left), the expression of CD44 versus Foxp3 within gated CD3$^+$CD4$^+$ T cells (middle), and the expression of CD44 and CD49d within gated CD3$^+$CD8$^+$ T cells (right) in the spleens of SPF and wildling mice. (**F**) Graphs depict quantities of total and naïve CD4$^+$ and CD8$^+$ T cells, effector CD4$^+$ T, Foxp3$^+$ T_{reg}, CD8 T_{VM}, and CD8 T_{TM} cells in the spleens of SPF and wildling mice, as indicated by gates in (E). (**G**) Spider plots of IFN-γ, IL-10, IL-4, IL-5, IL-13, and IL-17 secretion in splenocyte cultures of SPF (blue) and wildling mice (green) restimulated with heat-killed microbes in the presence or absence of MHC-II–blocking antibody. In (C) to (F), each dot represents one mouse. $n = 8$, and results are from one time-course experiment, and one-way ANOVA and Bonferonni's test were used to compare SPF mice and wildlings. In (G), $n = 5$, and one representative experiment of two is shown. Student's *t* test was used for comparisons. Means and SEM are depicted, $^*P < 0.05$, $^{**}P < 0.01$, $^{***}P < 0.001$, and $^{****}P < 0.0001$.

the effector T cell pool especially after 4 weeks of age, and wildling mice have a strong regulatory cytokine response to commensals.

Cytokine-producing effector CD4 T cells are prominent in the lungs of wildling mice

Asthma is an allergic disease of the lung parenchyma and airways and is typified by the presence of T_H2 cells, which secrete IL-4, IL-5, and IL-13 (*27*). To analyze the T helper cell composition of adult SPF and wildling mice, we restimulated lung and lung-draining mediastinal lymph node (medLN) cells with phorbol 12-myristate 13-acetate (PMA) and ionomycin for 3 hours in vitro. Thereafter, cytokine production was assessed in gated populations by flow cytometry. T_H1 (IFN-γ^+), T_H2 (IL-13$^+$), and T_H17 (IL-17$^+$) cells were observed in greater abundance in the lungs and medLNs of wildlings compared with SPF mice (Fig. 2A and fig. S3A). In addition, wildlings had much higher quantities of IL-10–producing classical Foxp3$^+$ T_{reg} cells and IL-10$^+$ Foxp3$^-$ effector CD4 T cells, sometimes referred to as type 1 regulatory cells (Fig. 2B and fig. S3A). Thus, wildlings have inflated populations of not only putative inflammatory but also anti-inflammatory CD4 T cells at resting.

T_H2 cells accumulate in the wildling mouse lung over time

To analyze more precisely when T_H2 cells emerged in the wildling mouse lung, we analyzed GATA3 expression alongside ST2 (a subunit of the IL-33R) in effector CD4 T cells from postnatal day 5 to day 98 (Fig. 2C). T_H2 cells (GATA3$^+$Foxp3$^-$ effector CD4 T) were already present at a significantly higher frequency in wildling lung 14 days postnatal (Fig. 2C). Numerically, T_H2 cells were present in larger quantities at 28 days postnatal and continued to expand markedly to levels approximately fivefold higher than that observed in SPF mice at day 98 (Fig. 2C). A large proportion of GATA3$^+$ T_H2 cells in wildlings also expressed ST2 and the tissue residency marker CD69 (Fig. 2C and fig. S3B). In comparison, the frequency and number of GATA3$^+$Foxp3$^+$ T_{reg} cells, which have been shown to play roles in regulating tissue immunity (*28*, *29*), were not different in wildlings and SPF mice at any time point (Fig. 2C).

Type 2 innate lymphoid cells (ILC2) have the ability to produce IL-5 and IL-13 (*30*) and outnumber T_H2 cells by 9:1 in most nonlymphoid tissues, including lung, adipose tissue, and skin (*31*). Moreover, it has been noted that ILC2 infiltrate the mouse lung 10 to 14 days postnatal and stabilize after weaning (*32*). ILC2 indeed appeared to increase in the lungs of SPF mice between days 5 and 14, but this accumulation was significantly less prominent in wildlings (Fig. 2D). By day 28, numbers of lung ILC2 were comparable between groups; however, the frequency of ILC2 was lower in wildlings at day 98 (Fig. 2D). In the bone marrow, hematopoietic progenitors were largely comparable across time points

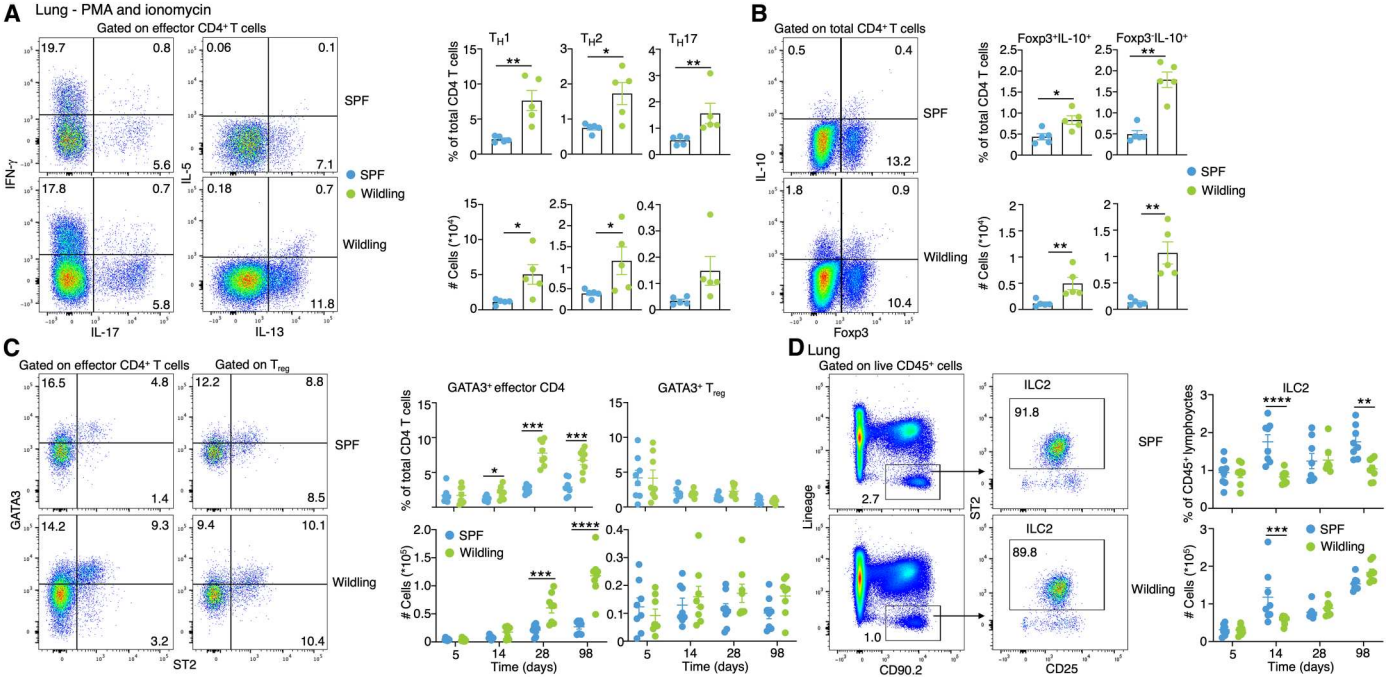

Fig. 2. A population of GATA3$^+$ST2$^+$ T_H2 cells is prominent in the wildling lung. (**A**) Representative flow plots of IL-17 versus IFN-γ and IL-13 versus IL-5 expression on gated CD44$^+$Foxp3$^-$ effector CD4 T cells in the lungs of adult (9 to 10 weeks of age) SPF and wildling mice. Bar graphs depict the percentage and number of T_H1 (IFN-γ^+), T_H2 (IL-5$^+$ and/or IL-13$^+$), and T_H17 (IL-17$^+$) cells. (**B**) Representative flow plots of Foxp3 versus IL-10 expression on gated CD4 T cells in the lungs of SPF and wildling mice and the corresponding frequency and number of Foxp3$^+$IL-10$^+$ and Foxp3$^-$IL-10$^+$ cells. (**C**) Representative flow plots of ST2 versus GATA3 on gated effector CD4 T cells and on gated T_{reg} cells. Graphs show the percentage and absolute number of GATA3$^+$ T_H2 and GATA3$^+$ T_{reg} in the lungs of unmanipulated SPF and wildling mice at days 5, 14, 28, and 98 after birth. (**D**) Representative flow plots of CD90.2 versus lineage markers (CD3, Gr-1, CD19, CD11c, and NK1.1) and CD25 versus ST2 cells in the lungs of SPF and wildling mice. Bar graphs depict the frequency and absolute number of ILC2 in the lungs of unmanipulated SPF and wildling mice. In (A) and (B), $n = 5$, and one representative experiment of two is shown. Student's t test was used to compare wildling with SPF mice. In (C) and (D), one-way ANOVA and Bonferroni's multiple comparisons test were used for multiple comparisons, $n = 8$, and results are from one time-course experiment. Means and SEM are depicted, *$P < 0.05$, **$P < 0.01$, ***$P < 0.001$, and ****$P < 0.0001$.

with some notable exceptions (fig. S4, A and B). For instance, at day 28 after birth, there was a reduction in common lymphoid progenitors in wildlings, whereas in 98-day-old mice, precursor ILC2 were increased in wildling bone marrow (as a proportion of $CD45^+$ cells) (fig. S4B).

In all, wildling mice accumulate large populations of effector T cells over time at sites including the spleen, medLN, and lung. Although wildlings appear to harbor regulatory responses to commensals, they also contain higher levels of T_H2 cells with putative proallergic functions.

Wildling mice develop robust pathogenic inflammation in response to HDM

To analyze the response of wildlings to allergens, we exposed mice to extracts of house dust mite (HDM), a near-ubiquitous aeroallergen to which asthmatics are commonly sensitive (*33*–*35*). In HDM-allergic asthmatics, HDM induces the production of cytokines, including IL-4, IL-5, and IL-13, from T_H2 cells and antibody production by B cells and promotes inflammation and mucus deposition in the airways (*27*). HDM (1 μg) was administered intranasally on day 0 and followed by five daily administrations of 10 μg of HDM on days 7 to 11. On day 15, mice were sacrificed, and airways, lung tissue, lung-draining medLN, and serum were analyzed for signs of inflammation (Fig. 3A). HDM administration led to a large influx of cells into the airways of wildling and SPF mice (Fig. 3B). Lung and medLN cellularity were highest in wildlings administered HDM compared with corresponding SPF mice (Fig. 3B). Wildlings developed robust airway eosinophilia and had significantly higher numbers of eosinophils in lung tissue (Fig. 3, C and D), indicative of heightened type 2 immune responses. Elevated numbers of T and B cells were also present in lung tissue and bronchoalveolar lavage fluid (BALF) samples collected from wildling mice, suggesting that wildlings developed a strong inflammatory response to HDM (Fig. 3, C and D). HDM administration into SPF or wildling mice induced a marked inflammation surrounding the airways with signs of epithelial thickening, as assessed by hematoxylin and eosin (H&E) staining (Fig. 3, E and F). In addition, goblet cells were also more prominent in HDM-administered wildlings compared with SPF mice when sections were analyzed by periodic acid–Schiff stain (PAS; Fig. 3, G and H). HDM induced strong antigen-specific serum IgG1 in both SPF mice and wildlings but negligible antigen-specific serum IgE responses in this 2-week model of allergen challenge (Fig. 3I). Hence, the rich microbial exposures of wildling mice do not dampen and may instead promote some aspects of allergic inflammation.

T_H2 cell responses to HDM are heightened in wildlings compared with SPF mice

T cells are activated through highly diverse T cell antigen receptors (TCRs) expressed on their cell surface. Innate-like T cells including natural killer T (NKT), mucosal-associated invariant T (MAIT), and γδ T cells have restricted TCR gene usage and have been proposed to be affected by microbial exposures. We found reduced NKT cells and slightly higher MAIT cell numbers in lungs of wildlings administered with phosphate-buffered saline (PBS) compared with SPF mice (fig. S5, A to C). After HDM instillation, NKT, MAIT, and γδ T cells were similarly reduced in the lungs of SPF mice and wildlings (fig. S5, A to C).

HDM is known to induce the differentiation of CD4 T cells into T_H2 cells, which express ST2 and secrete IL-5 and IL-13 in the lung (*36*). We analyzed the T_H2 cell response in wildlings in several ways. First, single-cell suspensions from BALF, lung, and medLN were assessed for cytokine production after mitogenic stimulation with PMA and ionomycin. Wildlings consistently had more vigorous T_H2 cell responses than SPF mice across the BALF, lung tissue, and medLN (Fig. 4B and fig. S6, A to C), with approximately 40% of gated effector ($CD44^+Foxp3^-$) CD4 T cells in the BALF producing IL-13 and/or IL-5 (Fig. 4A and fig. S6A). T_H1 (IFN-γ^+ effector CD4) and T_H17 (IL-17^+ effector CD4) cells were also increased in absolute numbers in BALF, lung tissues, and medLNs of wildling mice (Fig. 4B and fig. S6, A to C). No obvious difference in the number of germinal center B cells was observed between SPF mice and wildlings after HDM exposure (fig. S6F).

In cultures of lung cells with HDM extracts, the overall number of T_H2 cells detected in wildlings exposed to HDM was increased compared with HDM-exposed SPF mice (Fig. 4C and fig. S6D). HDM-exposed wildlings also had higher numbers of T_H17 and T_H1 cells in lung cultures with HDM, although their frequency was not significantly increased compared with PBS-exposed mice (Fig. 4C and fig. S6D).

To analyze the response to HDM at the epitope-specific level, the levels of Der p $1_{(217–227)}$–restricted lung CD4 T cells were assessed by tetramer staining. In mice exposed to HDM, Der p 1:I-A^b tetramer–reactive cells were expanded and comparable in number between SPF and wildling mice (Fig. 4, D and E). However, Der p 1:I-A^b tetramer–reactive cells in wildlings were composed of a higher frequency of T_H2 cells ($ST2^+$) and a reduced frequency of T_{reg} ($Foxp3^+$) compared with their SPF counterparts (Fig. 4, D and E).

Wildling mice have robust T_{reg} cell responses after HDM exposure

T_{reg} cells are pivotal to regulating inflammatory responses, and in recent years, $ST2^+$ T_{reg} cells have been proposed to play important roles in regulating inflammation in adipose tissue, the colon, muscles, and in lung allergic responses (*37*–*40*). We analyzed Foxp3 alongside ST2 expression within the CD4 T cell pool after HDM exposure. Proportionally, $ST2^+$ conventional CD4 T cells were increased, whereas $ST2^+$ $Foxp3^+$ T_{reg} were lower in wildlings, in line with the strong T_H2 cell response observed (Fig. 4F and fig. S6E). Nonetheless, HDM still induced expansion of the T_{reg} cell pool, including those bearing ST2, in the airways and lung tissues of wildlings (Fig. 4F and fig. S6E).

Overall, de novo responses to HDM, as measured by Der p 1:I-A^b tetramer, appeared to be similar between wildlings and SPF mice. However, the overall T_H2 cell response, which may include endogenous "bystander" T_H2 cells, was noticeably larger in wildlings than in SPF mice.

Prolonged HDM exposure induces comparable pathological responses in SPF mice and wildlings

Because allergen exposure in the human population is often persistent, we tested the response of SPF mice and wildlings in a prolonged model of allergen exposure. HDM was administered over a period of 6 weeks (sensitization on day 0 and HDM three times weekly from day 7), and the inflammatory response was measured 4 days after the final allergen administration (Fig. 5A). SPF mice and

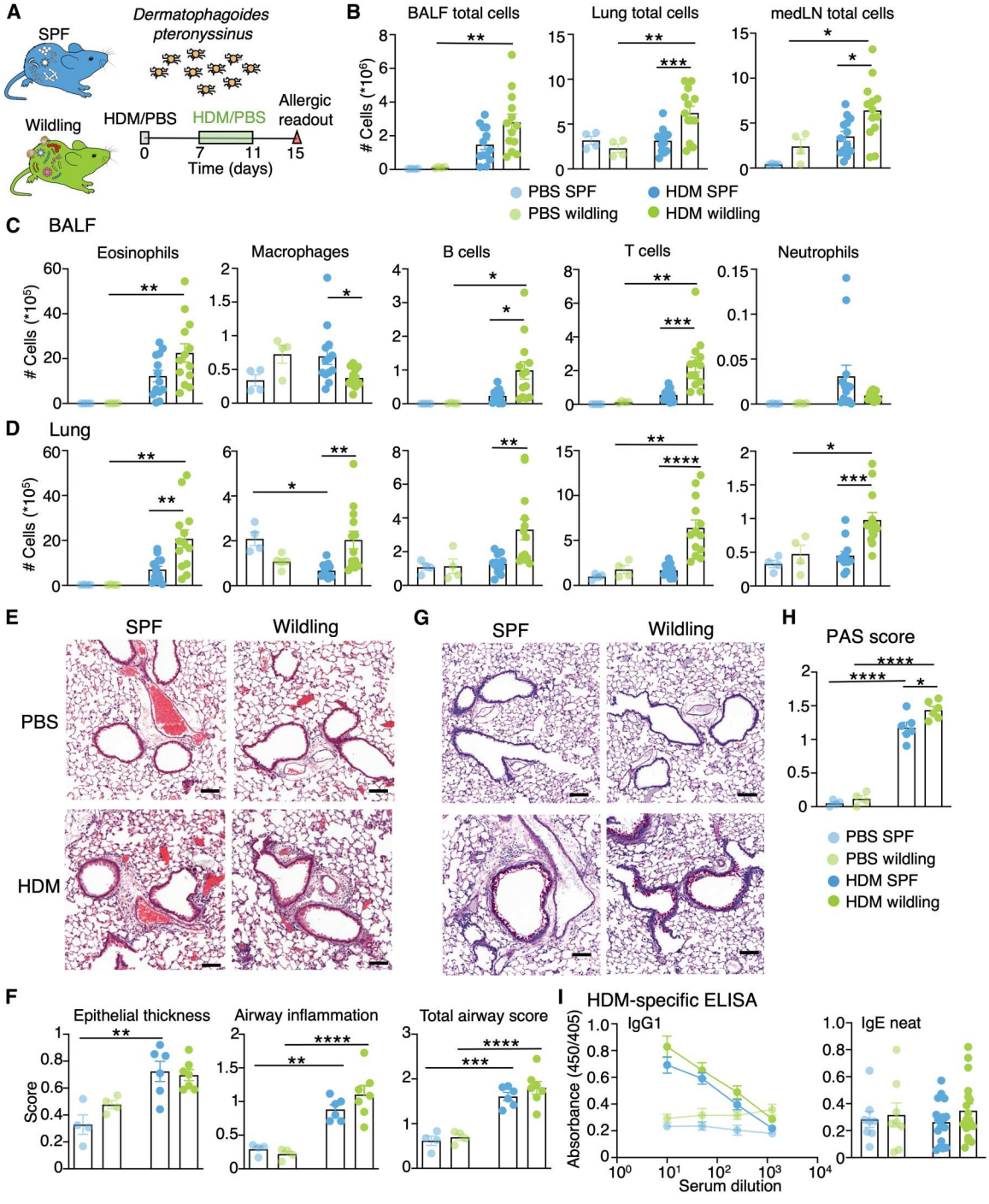

Fig. 3. Wildling mice develop robust allergic inflammation after administration of HDM. (**A**) Regimen of HDM instillation into the airways and analysis at day 15. (**B**) Graphs depict total cells in the BALF, lungs, and medLNs of SPF and wildling mice. (**C** and **D**) Bar graphs depict the total number of eosinophils (Siglec-F$^+$CD11c$^-$), alveolar macrophages (Siglec-F$^+$CD11c$^+$), B cells (Siglec-F$^-$CD11c$^-$B220$^+$), T cells (Siglec-F$^-$CD11c$^-$CD3$^+$), and neutrophils (Siglec-F$^-$CD11c$^-$Gr-1$^+$) in the BALF and lungs of SPF and wildling mice, as measured by flow cytometry. (**E**) Representative H&E and (**G**) PAS-stained lung tissue from SPF and wildling mice administered PBS/HDM. Scale bars, 100 μm. (**F**) Statistical analysis of epithelial thickness, airway inflammation, and total airway (epithelial thickness + airway inflammation) scores as quantified by H&E. (**H**) Statistical analysis of mucus content as quantified by PAS scores. All slides were scored in a blinded fashion. (**I**) Serum IgG1 and IgE specific to HDM was quantified by ELISA. One-way ANOVA and Bonferroni's multiple comparisons test were used. In (A) to (D), mice administered PBS $n = 4$ and mice administered HDM $n = 13$ were pooled from two experiments. In (E) to (H), PBS $n = 4$ and HDM $n = 6$ and 7 from one experiment. In (I), PBS $n = 8$ pooled from two experiments and HDM $n = 18$ and 19 pooled from three experiments. *$P < 0.05$, **$P < 0.01$, ***$P < 0.001$, and ****$P < 0.0001$.

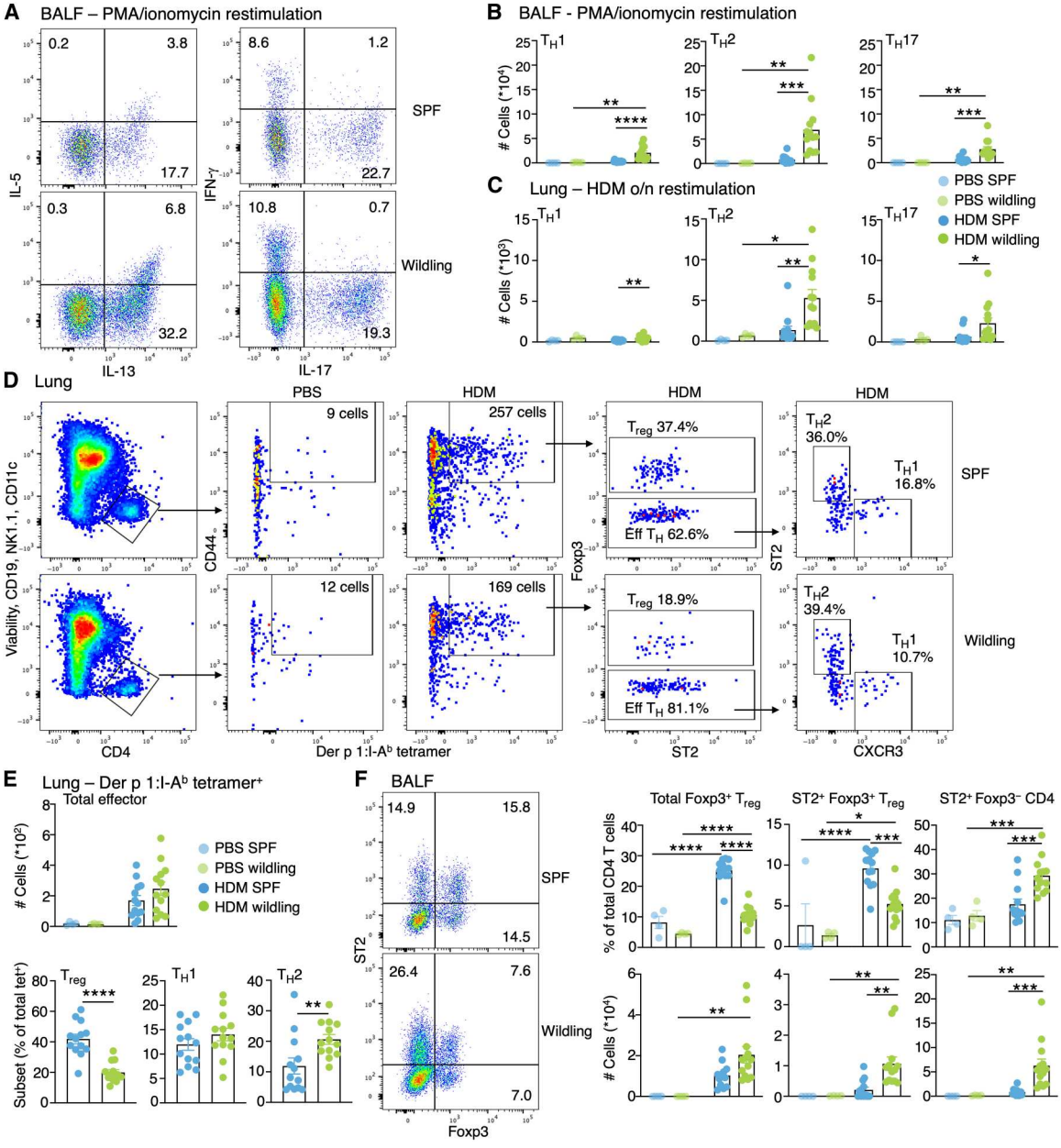

Fig. 4. T_H2 cell responses are augmented in wildlings after HDM administration. (**A**) Representative flow plots of IL-13 versus IL-5 (left) and IL-17 versus IFN-γ (right) in gated effector $CD4^+$ T cells ($CD4^+CD44^+Foxp3^-$) after stimulation with PMA and ionomycin in the BALF of SPF and wildling mice. (**B**) Enumeration of T_H1 (IFN-γ^+), T_H2 (IL-13^+ and/or IL-5^+), and T_H17 (IL-17^+) cells after stimulation with PMA and ionomycin in the BALF of SPF and wildling mice. (**C**) Enumeration of T_H1, T_H2, and T_H17 cells after overnight (o/n) stimulation with HDM extracts in the lungs of SPF and wildling mice. (**D**) Gating strategy to identify Der p 1:I-A^b tetramer–reactive effector CD4 T cells in the lungs of SPF and wildling mice administered PBS or HDM. Foxp3 distinguishes cells that are T_{reg}, ST2 distinguishes T_H2 cells, and CXCR3 pinpoints T_H1 cells, as depicted. (**E**) Enumeration of total Der p 1:I-A^b tetramer$^+$ effector CD4 T cells and subsets therein in lung parenchyma. Because of low numbers in PBS mice, subset data were omitted from these groups. (**F**) Representative flow plots of Foxp3 versus ST2 expression on gated total CD4 T cells. Bar graphs show the percentage and number of total $Foxp3^+$ T_{reg}, $ST2^+$ $Foxp3^+$ T_{reg}, and $ST2^+$ $Foxp3^-$ conventional CD4 T cells. Student's *t* test was used to compare subset frequencies. One-way ANOVA and Bonferroni's multiple comparisons test were used for multiple comparisons. In analyzing T_{reg}, T_H1, and T_H2 subset proportions in (E), Student's *t* test was used. PBS $n = 4$ and HDM $n = 13$ pooled from two independent experiments. *$P < 0.05$, **$P < 0.01$, ***$P < 0.001$, and ****$P < 0.0001$.

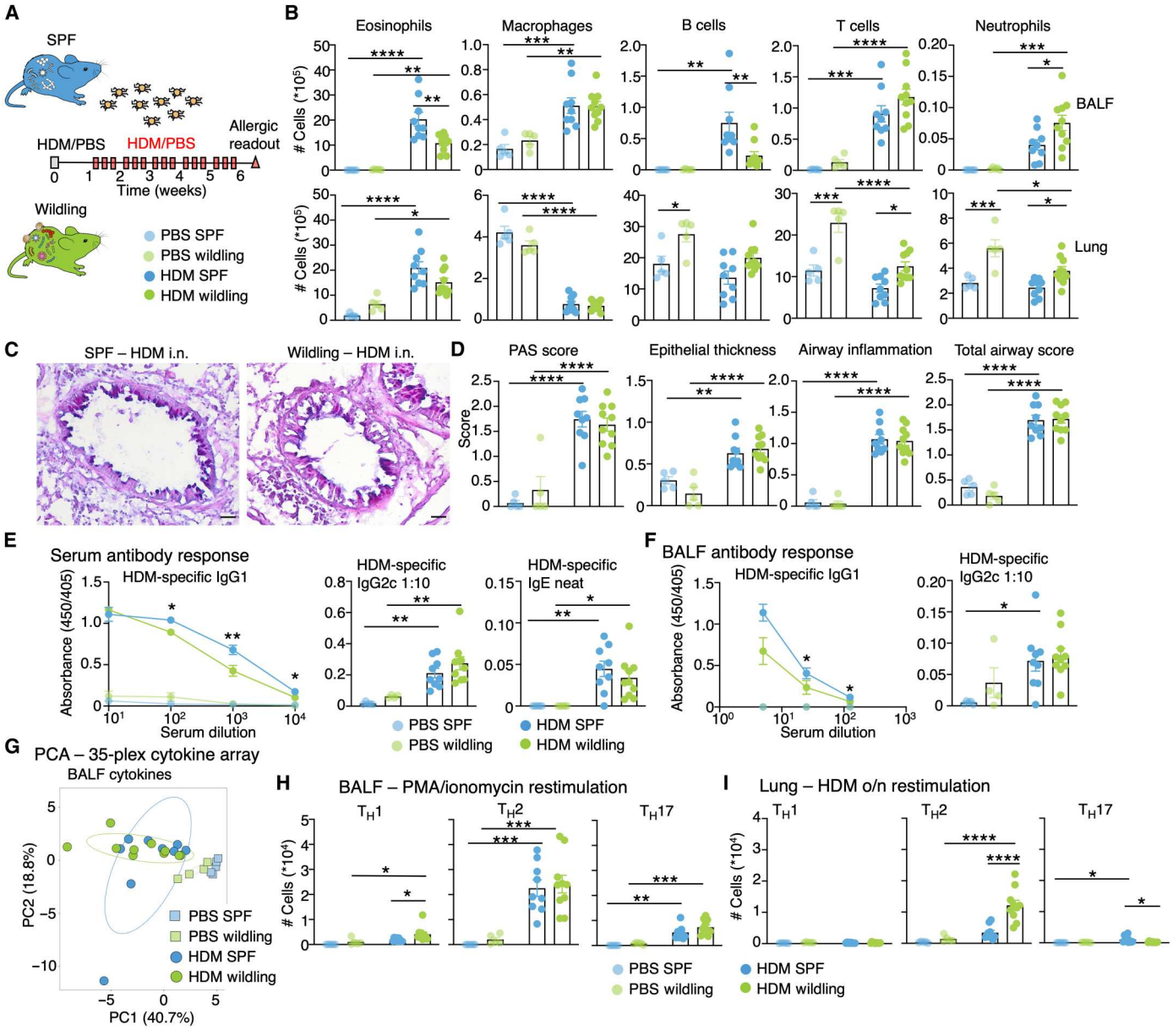

Fig. 5. Wildlings continue to generate robust T_H2 cell responses and associated allergic pathology after prolonged exposure to HDM. (**A**) Regimen of HDM/PBS instillation into the airways and analysis at day 46. (**B**) Bar graphs depict the total number of eosinophils, alveolar macrophages, B cells, T cells, and neutrophils in the BALF and lungs of SPF and wildling mice. (**C** and **D**) Representative PAS-stained lung tissue from an SPF and wildling mouse. Scale bars, 50 μM. Statistical analysis of mucus content was quantified by PAS scores and epithelial thickness, and airway inflammation and total airway scores were quantified by H&E. All slides were scored in a blinded fashion. i.n., intranasal. (**E** and **F**) Serum and airway HDM-specific IgG1, IgG2c, and IgE was quantified by ELISA. Airway HDM-specific IgE was undetectable. (**G**) Principal components analysis plot of 35-plex cytokine/chemokine panel on the BALF of SPF and wildling mice. (**H**) Enumeration of T_H1, T_H2, and T_H17 cells after PMA and ionomycin stimulation of BALF. (**I**) Enumeration of T_H1, T_H2, and T_H17 cells after stimulation overnight with HDM in the lungs of SPF and wildling mice. One-way ANOVA and Bonferroni's multiple comparisons test were used. In (B) to (I), mice administered PBS $n = 5$, and mice administered HDM, SPF $n = 9$ and wildling $n = 10$. *$P < 0.05$, **$P < 0.01$, ***$P < 0.001$, and ****$P < 0.0001$.

wildlings continued to show robust airway inflammation over this longer period of exposure, but some differences in airway cell composition were noted. For instance, wildlings had approximately half the number of airway eosinophils as compared with SPF mice, whereas a significant reduction in airway B cells was also noted in wildlings (Fig. 5B). Despite these differences, goblet cell metaplasia, epithelial thickening, and airway inflammation were all evident to a similar extent in SPF mice and wildlings (Fig. 5, C and D), suggesting that the wildling microenvironment had little impact on allergic pathology.

Subtle differences in the quality of the B and T cell response in wildlings with prolonged exposure to HDM

We analyzed the B cell response more closely after prolonged HDM exposure. The germinal center B cell response in medLN was comparable in SPF mice and wildlings (fig. S7D), indicating that the glandular B cell response was ongoing. However, circulating and airway HDM-specific IgG1 levels were significantly lower in wildlings (Fig. 5, E and F), in line with the reduction of B cells in the airways of these mice. No obvious skewing in HDM-specific antibodies toward or away from the IgG2c or IgE subclasses was observed (Fig. 5, E and F).

Analysis of the BALF with a 35-plex cytokine/chemokine panel showed substantial deviation of HDM-exposed wildling and SPF mice from those administered PBS (Fig. 5G and table S3). However, very few differences were observed between SPF mice and wildlings that had been administered HDM, with only MIP-2 (39.1 ± 7 versus 19.1 ± 2.8 pg/ml) and IL-10 (13.5 ± 2.3 versus 7.1 ± 0.9) being detected at significantly higher levels in BALF of wildling mice (table S3). Similar to the 2-week HDM exposure model, effector T_H2 cells were the most prominent cell population in BALF after prolonged HDM exposure (Fig. 5H and fig. S7A). After restimulation of lung cells overnight with HDM, wildlings still had the largest T_H2 cell response, whereas T_H1 and T_H17 cell responses were almost completely absent (Fig. 5I and fig. S7B). The T_{reg} cell response was reduced in wildling BALF compared with SPF mice (fig. S7C), whereas the lung tissue T_{reg} cell response was not expanded to the same extent as it was in the 2-week HDM model. Overall, wildlings maintained robust T_H2 cell responses after prolonged HDM exposure.

rIL-33 induces robust activation of endogenous T_H2 cells in wildlings

T_H2 cells generated in response to nematode infection have been shown to respond to nonspecific stimuli independently of their TCR (*41*–*43*). Given that wildlings had a substantially larger T_H2 cell pool at baseline and after HDM exposure, we analyzed the ability of these cells to respond to acute alarmin [recombinant IL-33 (rIL-33)] or allergen [*Alternaria alternata* (*Alt alt*) extract] exposure. The lung inflammatory response to rIL-33 was analyzed on day 2 (mice received rIL-33 only on days 0 and 1) and day 4 (mice received rIL-33 on days 0, 1, and 2) (Fig. 6A). SPF and wildling mice experienced a comparable infiltration of eosinophils into the lung and airways at days 2 and 4 after airway challenge with rIL-33 (Fig. 6B). The presence of goblet cells in airways was similar in SPF mice and wildlings after rIL-33 challenge (Fig. 6C). Analysis of airway inflammation with a 35-plex cytokine/chemokine panel showed a robust response in both wildlings and SPF mice administered rIL-33 at day 4 (Fig. 6D and table S4), hallmarked by high levels of IL-5 and IL-13. Although levels of airway IL-5 and IL-13 were similarly increased in SPF mice and wildlings, the quality of the cellular infiltration was different. T_H2 cells, identified as $ST2^{+-}$ $Foxp3^-$ CD4 T cells or by the expression of IL-13, were significantly higher in wildlings (Fig. 6E and fig. S8A). ILC2 and $ST2^+$ T_{reg} cells were significantly more prominent in the response of SPF mice to rIL-33 (Fig. 6E and fig. S8A), although both populations still expanded in wildlings. Similarly, extracts of *Alt alt*, a fungus with allergenic and proteolytic activity that drives vigorous ILC2 responses in SPF mice (*44*), induced early (day 2) T_H2 cell responses and a mild but significant goblet cell metaplasia specifically in wildlings (fig. S8, B to E).

To test whether T_H2 cells in wildlings could respond to rIL-33 independently of activation through the TCR, mice were administered an MHC-II–blocking monoclonal antibody (M5/114) on days −1 and 1. This had no effect on the levels of eosinophils or T_H2 cells in the airways or lung tissue of wildling mice (Fig. 6F), despite the ability of MHC-II blockade to block naïve OT-II cell activation in a similar system (fig. S9). Thus, the pathological response to rIL-33 administration is comparable in wildlings and SPF mice, but wildlings are marked by robust T_H2 cell responses, which are typically absent in conventional laboratory mice.

Antiparasitic treatment of wildlings does not dampen pathological responses to allergens

Because wildlings are colonized by a broad array of pathogens including pinworms and some ectoparasites, we analyzed the impact of antiparasitics (ivermectin and albendazol) on the inflammatory response to HDM and rIL-33 in a cohort of mice (fig. S10A). In response to HDM, antiparasitics appeared to have no effect on airway inflammation in wildlings, and the quality of the lung T_H cell response remained unchanged (fig. S10B). Similarly, in mice challenged with rIL-33, the airway cellular response was robust in SPF and wildling mouse lung, regardless of antiparasitic treatment. Some reduction was observed in the lung effector T cell response of wildlings treated with ivermectin and albendazol, particularly of T_H2 cells, yet this did not prevent a robust goblet cell response in these mice (fig. S10C).

In all, despite markedly different living conditions, high microbial exposures, and regulatory responses to commensals, wildlings develop vigorous allergic responses to common physiological allergens. In addition to the normal development of de novo T_H2 cell and antibody responses, an endogenous pool of lung T_H2 cells in wildlings responds rapidly and vigorously in short-term models of allergen or alarmin instillation, in a manner that appears independent of MHC-TCR interactions.

DISCUSSION

Allergies are known to be hereditary (*2*), but genetics alone cannot explain the surge in allergic diseases over the past century. Studies in laboratory mice have compared the allergic immune response of GF mice with those of SPF mice, noting that in the complete absence of microbes, T_H2 cytokines and IgE levels are increased, while anaphylactic responses to ingested antigens and airway inflammation to inhaled antigens are heightened (*15*–*17*). One may have expected that exposing SPF mice to a greater breadth of microbes would have the opposite effect. Yet wildlings developed robust signs of pathological inflammation with no obvious deviation away from T_H2 cell responses, and the balance of antibody subclasses was not obviously altered, despite a reduction in B cell response in wildlings over time.

What then were the features of the allergic immune response in wildlings that stood apart from SPF mice? Mostly, it was the rapid expansion of the lung T_H2 cell compartment in wildlings challenged with HDM over 2 weeks and in short challenges with rIL-33 or *Alt alt*. Recent studies have shown that tissue-resident T_H2 cells can respond to secondary challenges in a TCR-independent manner, but this mode of activation is not commonly emphasized,

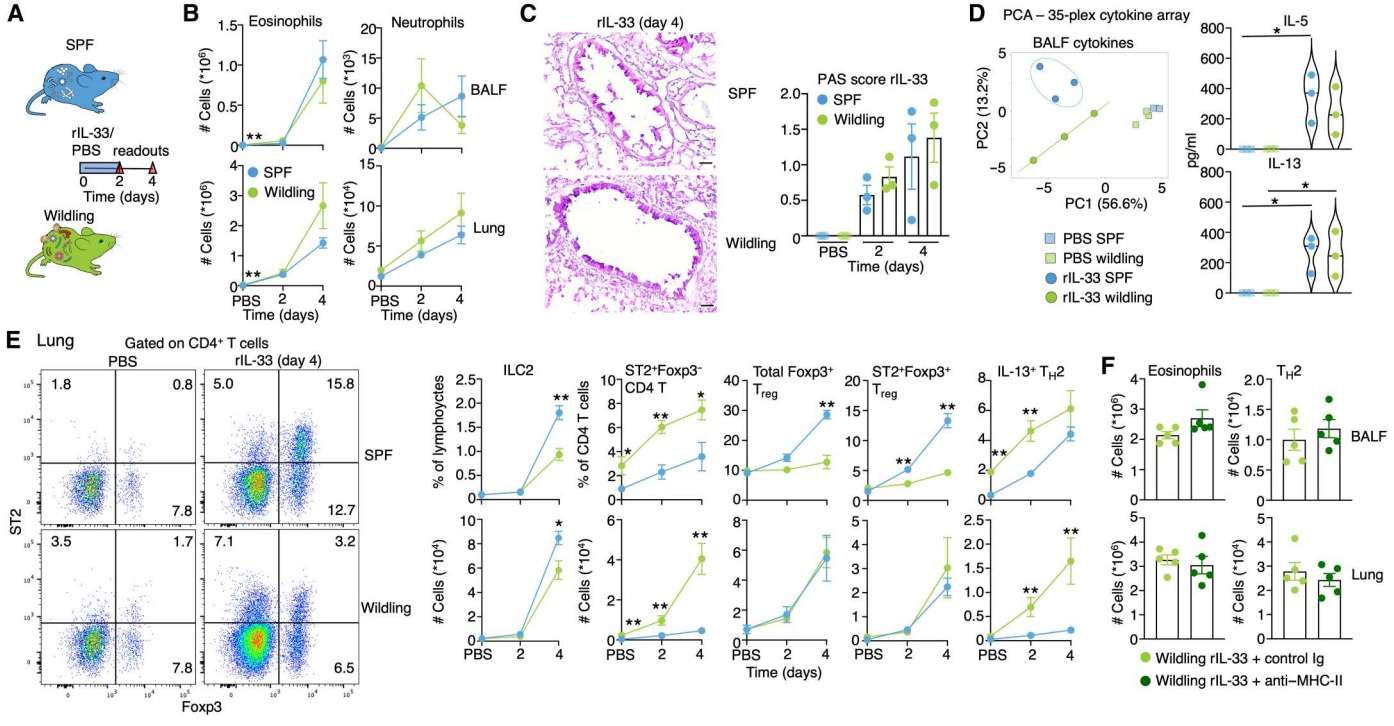

Fig. 6. An endogenous pool of T_H2 cells in wildlings responds to alarmin instillation. (**A**) Regimen of rIL-33 (200 ng daily for three consecutive days) or PBS instillation into mouse airways and subsequent analysis. (**B**) Graphs of eosinophil (Siglec-F$^+$CD11c$^-$) and neutrophils (Siglec-F$^-$CD11c$^-$Gr-1$^+$) in the airways and lung parenchyma of SPF and wildling mice. (**C**) Representative PAS-stained lung tissue from an SPF and wildling mouse from day 4 after initial challenge with rIL-33 and statistical analysis of mucus content as quantified by PAS scores. Scale bars, 50 μm. Slides were scored in a blinded fashion. (**D**) Principal components analysis plot of 35-plex cytokine/chemokine panel and the level of individual cytokines IL-5 and IL-13 in the BALF of SPF and wildling mice. (**E**) Representative plots of Foxp3 versus ST2 on gated CD4 T cells. Graphs show percentage and number of ILC2, ST2$^+$Foxp3$^-$ conventional CD4 T cells, total Foxp3$^+$ T_{reg}, ST2$^+$ Foxp3$^+$ T_{reg}, and T_H2 (IL-13$^+$ effector CD4 T) cells in the lung after administration of rIL-33 or PBS. (**F**) Wildling mice were administered rIL-33 as shown in (A) but on days −1 and 1 were injected with 500 μg of anti–MHC-II or control Ig. Graphs of eosinophils and T_H2 cell numbers in the BALF and lungs of wildling mice at day 4. In (B) and (E), $n = 6$ mice per group per time point pooled from two independent experiments. In (C), $n = 3$ mice per group per time point. In (F), $n = 5$ mice per group from one experiment. One-way ANOVA and Bonferroni's multiple comparisons test were used for multiple comparisons in (D). Student's t test was used for comparisons in (B), (C), (E), and (F), $^*P < 0.05$ and $^{**}P < 0.01$.

potentially because of the lack of effector cells found in sanitized mice. Some studies showed that TCR-independent activation of T_H2 cells provided protective immunity to secondary infections (*41* , *43*), while another proposed that they could drive pathogenic allergic responses (*42*). It remains unclear whether this mode of activity is responsible for sustaining inflammatory pathologies in human diseases such as asthma, atopic dermatitis, inflammatory bowel disease, or psoriasis, but wildlings, with their inflated pools of effector/memory T cells, provide a platform to test this possibility.

One possible implication of having an endogenous T_H2 cell population was that this would create competition for IL-33 availability and compromise ILC2, ST2$^+$ T_{reg}, or de novo generation of T_H2 cells. However, we found little evidence that endogenous T_H2 cells severely affected on the responsiveness of these populations, in line with the notion that tissue lymphocyte niches can expand to accommodate new responders (*45*, *46*).

In a recent study in which SPF mice were co-housed with pet store mice, ILC2-mediated allergic inflammation was found to be blunted soon after co-housing (*47*). However, the authors did note that at some point between 2 weeks and 2 months of co-housing, the protective effect was lost, and this correlated with a diminished type I IFN response. This implies that an active infection can subdue allergic responses. It also highlights a key difference between the co-housing and wildling approach, namely, that although wildlings are colonized by a greater magnitude and breadth of microbes, they are not "suddenly" infected as adults in the same manner as co-housed mice. In our analysis of BALF, no significant differences in the levels of IFNα or IFNβ were found between SPF mice and wildlings, which could indicate that the mice were healthy or that the type I IFN response is regulated differently in wildlings. It also brings to light a broader question: If microbial factors do regulate allergic disease in humans, is it by constant infection and reinfection in perpetuity or by altering our capacity to respond to allergens for extended periods of time?

One reason we used wildlings was because they are exposed to microbes and microbe-induced metabolites from birth. Early-life exposures have, in particular, been associated with regulating allergic immune responses in humans (*9*, *48*, *49*). Several studies have suggested that early gut colonization by *Lactobacilli* spp may suppress allergic sensitisation (*26*, *50*, *51*), through mechanisms including the production of short chain fatty acids (*52*, *53*) and the induction of IL-10 and T_{reg} cell responses (*54*, *55*). Thus, we assumed that wildlings, having had these early exposures and displaying regulatory responses to several commensals, may be capable of regulating immune responses to allergens for an extended

window of time. This was not the case and serves to question whether microbial exposures can exert long-lasting suppressive effects over allergic sensitisation and inflammation.

Our study does not rule out that microbes regulate allergic inflammation, because there is incontrovertible evidence that they can exert such effects. Some intestinal nematode infections and gut and lung commensals have been shown to dampen allergic inflammation (*56*–*58*). Thus, perhaps, microbes with important anti-inflammatory functions were absent from our wildling colony.

Rather than deciphering specific mechanistic contributions of single organisms, our study aimed to assess the impact of diverse and lifelong microbial exposures on the development of allergic inflammation. In a recent iteration of the hygiene hypothesis, it has been claimed that diverse microbial exposures are likely to make us more tolerant to incoming allergens, the so-called biodiversity hypothesis (*59*). Strong support for this hypothesis comes from epidemiological and intervention studies in Finland (*59*). Biodiversity is a complex concept that acknowledges microorganisms of all kingdoms—not just bacteria—that communicate with their respective host(s) and with each other in a multifactorial and nonlinear fashion (*60*–*62*). Nonbacterial constituents of the microbiome, including protists (*63*), parasites (*64*), fungi (*65*), and viruses (*66*), have important impacts on host physiology, as recently reviewed (*67*). Both humans and wildlings have a diverse virome and mycobiome, are also colonized with protists (*21*), and even "modern humans" living under supposedly hygienic conditions are, like wildlings, in frequent contact with parasites such as the pinworm *Enterobius vermicularis* (*68*, *69*). Thus, wildlings have a considerably more diverse microbial pool than SPF mice. Why the biodiversity of wildlings was unable to protect against allergic inflammation is unclear, but we did attempt to address the impact of parasites on the allergic response, because pinworms were shown to aggravate allergic responses to ovalbumin and autoantigens (*70*, *71*). Antiparasitics did not greatly alter the pathogenic immune response in wildlings, even if the T_H2 cell response to rIL-33 was somewhat subdued. It may be that elimination of fungi, which are generally thought to aggravate allergic immune responses (*72*), would affect the quality of allergic responses, but relative contributions of different microbial inputs and the role of biodiversity per se will need to be clarified in subsequent studies.

Some caveats of our study are worth noting. First, we only examined allergic immune responses after aeroallergen challenge. Other routes of antigen exposure including through the skin or gut may have revealed protective phenotypes of wildlings that were not evident in our assays. Altering the timing of allergen exposure, for instance, by instilling allergens in the first week(s) of life or sensitizing females before/during pregnancy may have uncovered periods when wildlings were protected from allergic sensitization. Moreover, potential benefits of the wildling microbiota may only reveal themselves when nonmicrobial and lifestyle factors known to influence allergy are incorporated into our models. For instance, unhealthy diets, decreased physical activity, and environmental pollutants, which are all thought to play a role in the rise in allergy incidence over the past century (*73*–*76*), may play greater or lesser roles in microbe-rich versus microbe-poor environments.

Thus, in this study, we demonstrate that despite high microbial exposures from birth, wildling mice mount robust responses to common aeroallergens, in contrast to what might have been predicted from preclinical mouse studies and observations in the human population. Future work is required to decipher if/when/how lifelong exposures, such as those present in wildling colonies, can regulate pathogenic allergic immune responses.

MATERIALS AND METHODS

Study design

The aim of this study was to analyze the impact that lifelong microbial exposures may have on the ability of mice to generate immune responses to common environmental allergens. To this end, we compared allergic inflammatory responses in C57BL/6NTac SPF mice house under standard conditions with those of C57BL/6NTac wildling mice housed under seminatural conditions. The microbial composition of SPF mice and wildlings was evaluated by next-generation sequencing, and the development of the lymphoid immune compartment over time was analyzed by flow cytometry. Short- and long-term regimens of intranasal instillation with HDM, *Alt alt* extracts, or the alarmin rIL-33 were tested. Pathological signs of allergic inflammation were evaluated by H&E and PAS staining of lung sections and scored in a blinded fashion. Immunological parameters of allergic inflammation were evaluated by flow cytometry of lung and lymphoid tissue and by enzyme-linked immunosorbent assay (ELISA) for cytokines and antibodies. Group sizes in experiments were based on the knowledge of variability in allergen models and in assays from our previous studies. All experiments were conducted in accordance with the Stockholms Norra djurförsöksetiska nämnd.

Mice

C57BL/6NTac murine pathogen–free (MPF) mice were used in all experiments and adhered to our characterization of SPF. C57BL/6NTac wildling mice were created through inverse GF rederivation as described by Rosshart and colleagues (*21*). The wildling mouse colony was housed and animals were bred at the Medical Center–-University of Freiburg, Germany. Ontogeny experiments presented in Figs. 1 and 2 were conducted at Medical Center–University of Freiburg, Germany. For experiments in allergen models, C57BL/6NTac wildlings and C57BL/6NTac MPF (SPF) mice were transported at the same time to the Comparative Medicine animal facilities at Karolinska Institutet and allowed to rest for at least 1 week before the commencement an experiment. Wildling and C57BL/6NTac MPF mice were around 8 to 12 weeks old at the start of allergy experiments and were always age-matched within experiments. Female mice were used in all experiments described herein. Experiments were approved by the Stockholm Regional Ethics Committee (8971/2017 + B6905/2020 and 3649-2019).

Assessment of the hygiene standards

For *C57BL/6NTac* mice, blood drops dried on Opti-Spot Cards (IDEXX BioAnalytics), dry fur swabs (DRYSWAB FLOCK from Puritan), dry oral swabs (FLOQSwabs from COPAN), and fecal pellets were collected according to the manufacturer's sampling guidelines and screened for microorganisms with two independent methods [polymerase chain reaction (PCR) and serology] using the "Mouse 3R Comprehensive Serology Panel" and the "Mouse 3R Quarantine Annual SOPF PCR Panel" from IDEXX BioAnalytics. The assays were performed on pooled samples; a microorganism was considered present if it was identified through at least one of the two independent methodologies.

For conventional specific pathogen-free *C57BL6/NTac* mice, the hygiene standard was assessed and reported by the mouse vendor (Taconic Biosciences). Hygiene status of the wildling facility is checked regularly and did not alter over the course of these experiments.

16*S* rRNA gene sequencing

Fecal samples were collected and stored at −20°C until processing. DNA was isolated with the Zymo Research 96-well DNA extraction Kit. Briefly, fecal samples were transferred into a 96-well bashing bead lysis rack, diluted with 650 μl of lysis buffer, and homogenized by Mini-BeadBeater-96 for 3 × 5 min. Samples were kept in ice for 5 min between bead beating steps. Subsequently, the homogenate was centrifuged at 4000*g* for 20 min. Four hundred microliters of the supernatant was transferred into a 2-ml 96-deep-well plate (Nunc) and centrifuged again for 20 min to thoroughly remove debris, particles, and beads. Two hundred microliters of the supernatant was used for DNA isolation and purification. Samples were purified using a 96-well Zymo Magkit on a TECAN Fluent Automation Workstation. 16*S* rRNA gene amplification of the V4 region (F515/R806) was performed according to an established protocol previously described (*77*, *78*). Briefly, DNA was normalized to 25 ng/μl and used as input for PCR with unique 12-base Golary barcodes incorporated via specific primers (obtained from Sigma-Aldrich). PCR was performed using Q5 polymerase (New England Biolabs) in triplicates for each sample, using PCR conditions of initial denaturation for 30 s at 98°C, followed by 25 cycles (10 s at 98°C, 20 s at 55°C, and 20 s at 72°C). After pooling and normalization to 10 nM, PCR amplicons were sequenced on an Illumina MiSeq platform via 250-bp paired-end sequencing.

Microbiome data were analyzed using the Usearch11 software package to assemble, filter, and cluster resulting reads. Sequences were filtered for low-quality reads and binned on the basis of sample-specific barcodes using QIIME v1.8.0 (*77*). Merging was performed using -fastq_mergepairs − with fastq_maxdiffs 30. Quality filtering was conducted with fastq_filter (-fastq_maxee 1), using a minimum read length of 250 bp and a minimum number of reads per sample = 1000. Reads were clustered into operational taxonomic units (OTUs) by open-reference OTU picking, and representative sequences were determined by use of the UPARSE algorithm (*79*). Abundance filtering (OTUs cluster > 0.5%) and taxonomic classification were performed using the RDP Classifier executed at 80% bootstrap confidence cutoff (*80*). Sequences without a matching reference dataset were assembled as de novo using UCLUST. Phylogenetic relationships between OTUs were determined using FastTree to the PyNAST alignment (*81*). The resulting OTU absolute abundance table and mapping file were used for statistical analyses and data visualization in the R statistical programming environment package phyloseq (*82*). Alpha diversity (richness and evenness) was estimated using the observed richness (number of different species directly observed in each sample) and the Shannon diversity index on the observed count values. For the following analysis, low abundant OTUs (corresponding to less than 0.5% of the abundance for all samples) were filtered out, and the OTU table was converted into relative abundance. Beta diversity was estimated using Bray-Curtis distances and visualized using principal coordinates analysis (PCoA). Community composition was examined at phylum and family level. Species belonging to the same family or phylum were aggregated together, and OTUs with no taxonomic annotation were categorized as "unknown."

Mycobiome sequencing

The internal transcribed spacer (ITS) samples were prepared following the manufacturer's instructions using the Quick-ITS Plus NGS Library Prep Kit (catalog no. D6424-PS1). A total input of ~10 ng of DNA was used per sample. The PCR program (42 cycles) was performed according to the manufacturer's instructions. For sequencing, the same volume of each sample, normalized by quantitative PCR was pooled, cleaned up using magnetic beads, and submitted for sequencing.

Demultiplexed reads were processed with the Usearch 9 ITS protocol (https://drive5.com/usearch/manual/ex_miseq_its.html). Briefly, sequences were filtered for low-quality reads. Merging was performed using -fastq_mergepairs, with fastq_maxdiffs 30. Quality filtering was conducted with fastq_filter (-fastq_maxee 1), using a minimum read length of 250 bp and a minimum number of reads per sample = 1000. Reads were clustered into 97% ID OTUs by open-reference OTU picking, and representative sequences were determined by use of the UPARSE algorithm (http://dx.doi.org/10.1038/nmeth.2604). Abundance filtering (OTUs cluster > 0.5 %) and taxonomic classification were performed using the Sintax Classifier executed at 80% bootstrap confidence cutoff (https://doi.org/10.7717/peerj.4652). Sequences without a matching reference dataset were assembled as de novo using UCLUST. Phylogenetic relationships between OTUs were determined using FastTree to the PyNAST alignment (*81*). The resulting OTU absolute abundance table and mapping file were used for statistical analyses and data visualization in the R statistical programming environment package phyloseq (*82*).

Models

HDM (Dermatophagoides pteronyssinus)

Mice were anesthetized with isoflurane and sensitized with 1 μg of HDM (Stallergenes Greer) in 40 μl of PBS intranasally. Seven days after sensitization, mice were challenged with 10 μg of HDM for five consecutive days (2-week model) or three times per week for 5 weeks (prolonged exposure model). Mice were sacrificed, and organs were harvested 4 days after the last challenge. BALF was collected by three consecutive flushes of the airway with 1 ml of PBS. In experiments where BAL cytokines/chemokines were analyzed, the first flush of the airways was collected in low protein-binding Eppendorf tubes and centrifuged at 300*g*, and the supernatant was used to analyze the protein content. The cell pellet was added back into suspension with the subsequent BALF flushes.

rIL-33 or *Alt alt* extract

rIL-33 (200 ng) or *Alt alt* extracts (Stallergenes Greer, 20 μg) were administered intranasally for three consecutive days. Mouse BALF, lung tissue, and medLN were harvested on day 2 (1 day after the second dose of rIL-33 or *Alt alt*) and on day 4 (2 days after the last dose of rIL-33 or *Alt alt*). To block MHC-II, 500 μg of anti–MHC-II antibody (M5/114) or control Ig (anti-phyt IgG AFRC MAC 51) was injected intraperitoneally on days −1 and 1. In experiments where BAL cytokines/chemokines were quantified, BALF was obtained as described above.

Organ processing

The medLN, thymus, and spleen were pushed through 100 μM sieves in around 10 ml volume of 2% heat-inactivated fetal calf serum (FCS; Sigma-Aldrich) in PBS [fluorescence-activated cell sorting (FACS) buffer] to achieve single-cell suspensions. Femurs were flushed with cold FACS buffer using 23- to 25-gauge needles. Total spleen and bone marrow single cells were lysed of red blood cells (RBCs) using a hypotonic buffer. Cells were resuspended in either FACS buffer or tissue culture medium, depending on the requirement for restimulation. The lungs of mice in allergen models were also processed in the same way as described above because we have noted that enzymatic treatment can lead to severe cell loss in highly inflamed lungs.

For analysis of lungs at baseline (as reported in Fig. 4, A and B), lungs were cut into small pieces and incubated in RPMI with 20 mM Hepes, 2.5 mM L-glutamine, 1× nonessential amino acids (NEAA; Sigma-Aldrich), Liberase TL (0.5 mg/ml; Roche), and deoxyribonuclease I (20 μg/ml; Roche) for 45 min at 37°C and 150 rpm. The cell suspension was passed through a 21- and 26-gauge needle and washed with RPMI containing 10% FCS, 20 mM Hepes, 2 mM L-glutamine, 1× NEAA, 50 μM β-mercaptoethanol, and 2 mM EDTA. Erythrocytes were lysed with 1× RBC lysis buffer (eBioscience) and filtered through a 70-μm cell strainer. Lungs were not perfused in this study.

Restimulation of T cells

To detect cytokine production, cells were cultured in Iscove's modified Dulbecco's medium (IMDM) supplemented with penicillin/streptomycin, L-glutamine, β-mercaptoethanol (all from Invitrogen), 1× NEAA (Sigma-Aldrich), and 10% heat-inactivated FCS (Sigma-Aldrich). For restimulation with PMA (50 ng/ml) and ionomycin (5 μM), brefeldin A (Sigma-Aldrich) was added from the beginning of culture, and cells were harvested 3 hours later. For HDM-specific restimulation, cell suspensions were plated in a 48-well plate with HDM extracts (20 μg/ml). After 6 hours, brefeldin A was added to the culture, and after an additional 9-hour culture, cells were collected and stained with antibodies for FACS analysis. The eBioscience Fixation Kit was used when intranuclear staining of Foxp3 was performed.

Tetramer staining

I-A(b) HDM Der p 1 217-227 CQIYPPNVNKI (*83*, *84*) was ordered from the National Institutes of Health (NIH) Tetramer Core Facility. Half of the lung cells were resuspended in 250 μl of FACS buffer with anti-CD16/CD32 and rat and mouse serum (all in 1/100 dilution), mixed well, and incubated for 10 min at room temperature (RT). Then, the total volume was topped to 500 μl with FACS buffer, and 5 μl of phycoerythrin (PE)–labeled tetramer was added for 1 hour at RT. After incubation, the EasySep Mouse PE-Positive Selection Kit II (STEMCELL Technologies, catalog no.17666) was used to select PE-labeled tetramer cells. Briefly, cells were washed once with 10 ml of cold FACS buffer and resuspended in 250 μl of magnetic-activated cell sorting buffer (0.5% fetal bovine serum and 2 mM EDTA in PBS) with 25 μl of PE Selection Cocktail and incubated for 15 min at RT. Thereafter, 15 μl of Dextran RapidSpheres was added and incubated for an additional 10 min at RT. Cells were then washed and selected with magnets according to the manufacturer's protocol.

For CD1d-PBS-57 and MR1-5-OP-RU tetramer (from the NIH Tetramer Core Facility) staining, whole lung cells were incubated with tetramers in the presence of Fc block and rat and mouse serum for 30 min. Thereafter, cells were stained for other markers.

Flow cytometry

Flow cytometry was performed on a BD LSRII with combinations of the following antibodies: from BD Biosciences: CD19 (1D3), CD11c (HL3), B220 (RA3-6B2), CD3 (145-2C11), CD4 (RM4-5 and GK1.5), CD8 (53-6.7), CD44 (IM7), Gr-1 (RB6-8C5), IFN-γ (XMG1.2), IL-4 (11B11), IL-17 (TC11-18H10), Ki-67 (B56), CXCR3 (CXCR3-173), CD90.2 (53-2.1), CD45.2 (104), CD25 (PC 61), CD69 (H1.2F3), CD49d (R1-2), Siglec-F (E50-2440), Gata3 (L50 823), CD16 (2.4G2), TCRβ (H57 597), TCRγδ (GL3), CD62L (MEL-14), TCR Vβ 5.1/5.2 (MR9-4), Ter^{119} (TER-119), α4β7 (LPAM1) (DATK32), Sca-1 (D7), CD95 (Jo2), CD138 (281-2), and purified rat anti-mouse CD16/CD32 (2.4G2); from Invitrogen: CD127 (A7R34), CD11c (N418), GL-7 (GL7), Foxp3 (FJK-16s), and IL-13 (ebio13A); from BioLegend: IL-5 (TRFK5), NK1.1 (PK136), ST2 (DIH9), Thy1.2 (53-2.1), Flt3 (CD135) (A2F10), FcεRIα (MAR-1), CD117 (Ckit) (2B8), PD-1 (29F.1A12), CD26 (H194-112), CD172a (P84), XCR-1 (ZET), and CD103 (2E7); and from R&D Systems: IL17RB (752101). The CellTrace Violet Cell Proliferation kit from Thermo Fisher Scientific was used to track transferred OT-II cells. Fixable viability dye eFluor 780 or LIVE/DEAD Fixable Yellow Dead Cell Stain Kit from Thermo Fisher Scientific were used to assess viability. All samples were fixed before being run on the flow cytometer.

Histopathological analysis

In Fig. 2, independent mouse lungs were inflated with and fixed in 10% formalin for a minimum of 24 hours before being embedded in paraffin. Four-micrometer sections were cut on a rotary microtome (Mikrom HM355s). In Figs. 4 to 6, the right middle lobe was taken for histological analysis, whereas the other lobes were used for cellular analysis by flow cytometry. The right middle lobe was fixed in 4% paraformaldehyde for 24 hours and embedded in optimal cutting temperature and frozen at −80°C, and then 7-μm sections were cut on a Cryostar NX70 Cryostat (Thermo Fisher Scientific). PAS and H&E stains were performed. Slides were imaged on an Olympus IX70 inverted fluorescent microscope using 20× objective.

For analysis of mucus score, PAS-stained sections were scored on a 0- to 4-point scale with points assigned on the basis of the percentage of the airway covered by positively stained cells: 0 points for 0% of the airway affected, 1 point for 1 to 25%, 2 points for 26 to 50%, 3 points for 51 to 75%, and 4 points for more than 75% PAS positive. For analysis of epithelial thickness, 1 point was assigned for airways where the epithelium was not a monolayer and had >1 cell, and 1 point was assigned for the presence of clusters of airway epithelial cells. For assessment of inflammation around the airways, 0 points were assigned for no inflammation, 1 point for some inflammatory cells around airway, 2 points for a ring of inflammatory cells around the airway, 3 points for a ring two to four cells deep, and 4 points for a ring more than four cells deep.

Antibody ELISAs

HDM allergen extract (5 μg/ml) was diluted in PBS and incubated at 4°C overnight in a 96-well plate (nunc). For total IgM, IgE, IgG1, IgG2c, and IgA, plates were incubated at 4°C overnight with IgM-

UNLB (SouthernBiotech, catalog no. 1020-01), IgE-UNLB (BD Biosciences, catalog no. 553414), IgG1-UNLB (SouthernBiotech, catalog no. 1070-01), IgG2c-UNLB (SouthernBiotech, catalog no. 1079-05), IgA-UNLB (SoutherBiotech, catalog no. 1040-01). Plates were incubated at 4°C overnight and blocked with 2% milk in PBS the following morning. Serum/BALF was diluted as indicated. For detection of allergen-specific IgE, serum was depleted of IgG first using Protein G HP SpinTrap (Invitrogen) columns according to the manufacturer's protocol. Plates were washed in PBS/Tween. Serum/BALF was added to the wells and incubated for 2 hours at RT or overnight at 4°C. Plates were washed again and incubated for 1 hour with secondary antibody, either horseradish peroxidase (HRP)–coupled anti-IgG1 (Southern Biotech, 1070-05), anti-IgG2c (Southern Biotech, 1079-05), or biotin-coupled anti-IgE (BD, R35-72), anti-IgA (BD, 556978), and anti-IgM (Mabtech AB, 3845-6-250) followed by streptavidin-HRP (Mabtech). TMB substrate (KPL) followed by H_2SO_4 was used to develop and stop the reaction. The Asys Expert 96 ELISA reader (Biochrom) was used to read the optical density at 450 nm/405 nm.

Microbial restimulation assays

A single-cell suspension of splenocytes or medLN was prepared in complete IMDM medium at 5×10^6 and 2×10^6 cells/ml, respectively. One hundred microliters of cells was plated in 96-well round-bottom plates, and another 100 μl of medium containing heat-killed microbes (10^8 cfu/ml, 95°C for 15 min) or medium was added to the plates. Anti–MHC-II or control Ig (10 μg/ml) was added to the medium. The heat-killed microbes used were as follows: *Clostridium perfingens* (ACHIM3, 47-3), *S. aureus* [American Type Culture Collection (ATCC) 29213], *Candida albicans* (CCUG44135), *L. reuteri* (DSM 17938), *L. johnsonii* (CCUG30725), *S. typhimurium* (SL1344), *E. coli* (ATCC 35218), and *K. pneumoniae* (ATCC 25955). *S. aureus*, *E. coli*, and *K. pneumoniae* were provided by Å. Sjöling's group at Karolinska Institutet. Cell culture supernatants were collected after 48 hours and stored at −20°C.

Cytokine quantifications

In microbial restimulation assays, supernatant cytokines were measured using BD Flex Set kits in line with the manufacturer's protocol. Briefly, capture beads with anti-cytokine antibodies were incubated with supernatants for 2 hours and thereafter incubated a further hour with anti-cytokine PE detection reagent. Capture beads were analyzed by flow cytometry, and supernatant cytokine concentration was evaluated using GraphPad Prism software.

For measurement of cytokines and chemokines from BALF, a 29-plex U-PLEX assay and a customized 6-plex U-PLEX assay [Meso Scale Diagnostics (MSD)] including the following cytokines were used: eotaxin, granulocyte-macrophage colony-stimulating factor, IFN-α, IFN-β, IFN-γ, IL-1β, IL-2, IL-4, IL-5, IL-6, IL-9, IL-10, IL-12p70, IL-13, IL-15, IL-16, IL-17A, IL-17A/F, IL-17C, IL-17E/IL-25, IL-17F, IL-21, IL-22, IL-23, IL-27p28/IL-30, IL-31, IL-33, IFN-γ–induced protein 10 (IP-10), CXCL1, monocyte chemoattractant protein (MCP)–1, macrophage inflammatory protein (MIP)–1α, MIP-2, MIP-3α, RANTES, and tumor necrosis factor. The assay was performed according to the manufacturer's instructions using 50 μl BALF. The analysis was done using a QuickPlex SQ 120 instrument (MSD) and DISCOVERY WORKBENCH version 4.0 software.

Statistical analysis

The statistical analysis used is stipulated in each figure and was calculated using GraphPad Prism software. Student's *t* test was used to compare two groups. One-way analysis of variance (ANOVA) and Bonferroni's multiple comparisons test were used when more than two comparisons were made. In HDM experiments, statistical comparisons were made between SPF mice and wildlings administered PBS, SPF mice and wildlings administered HDM, and HDM-exposed SPF/wildling mice with their respective PBS control. For analysis of lymphocyte ontogeny in wildlings, SPF and wildlings were compared at the same time point, and corrections were made for the number of comparisons along the time course. Only significant comparisons are indicated. Mean and SEM are shown in all graphs. $^*P < 0.05$, $^{**}P < 0.01$, $^{***}P < 0.001$, and $^{****}P < 0.0001$.

Supplementary Materials

This PDF file includes:
Figs. S1 to S10

Other Supplementary Material for this manuscript includes the following:
Tables S1 to S4
Data file S1
MDAR Reproducibility Checklist

REFERENCES AND NOTES

1. L. Henriksen, J. Simonsen, A. Haerskjold, M. Linder, H. Kieler, S. F. Thomsen, L. G. Stensballe, Incidence rates of atopic dermatitis, asthma, and allergic rhinoconjunctivitis in Danish and Swedish children. *J. Allergy Clin. Immunol.* **136**, 360–366.e2 (2015).
2. C. Ober, T.-C. Yao, The genetics of asthma and allergic disease: A 21st century perspective. *Immunol. Rev.* **242**, 10–30 (2011).
3. T. A. E. Platts-Mills, The allergy epidemics: 1870-2010. *J. Allergy Clin. Immunol.* **136**, 3–13 (2015).
4. M. Kilpeläinen, E. O. Terho, H. Helenius, M. Koskenvuo, Farm environment in childhood prevents the development of allergies. *Clin. Exp. Allergy* **30**, 201–208 (2000).
5. M. J. Schuijs, M. A. Willart, K. Vergote, D. Gras, K. Deswarte, M. J. Ege, F. B. Madeira, R. Beyaert, G. van Loo, F. Bracher, E. von Mutius, P. Chanez, B. N. Lambrecht, H. Hammad, Farm dust and endotoxin protect against allergy through A20 induction in lung epithelial cells. *Science* **349**, 1106–1110 (2015).
6. O. S. Von Ehrenstein, E. Von Mutius, S. Illi, L. Baumann, O. Böhm, R. von Kries, Reduced risk of hay fever and asthma among children of farmers. *Clin. Exp. Allergy* **30**, 187–193 (2000).
7. E. von Mutius, C. Braun-Fahrländer, R. Schierl, J. Riedler, S. Ehlermann, S. Maisch, M. Waser, D. Nowak, Exposure to endotoxin or other bacterial components might protect against the development of atopy. *Clin. Exp. Allergy* **30**, 1230–1234 (2000).
8. E. von Mutius, The microbial environment and its influence on asthma prevention in early life. *J. Allergy Clin. Immunol.* **137**, 680–689 (2016).
9. M. Waser, K. B. Michels, C. Bieli, H. Flöistrup, G. Pershagen, E. von Mutius, M. Ege, J. Riedler, D. Schram-Bijkerk, B. Brunekreef, M. van Hage, R. Lauener, C. Braun-Fahrländer; PARSIFAL Study team, Inverse association of farm milk consumption with asthma and allergy in rural and suburban populations across Europe. *Clin. Exp. Allergy* **37**, 661–670 (2007).
10. S. F. Bloomfield, R. Stanwell-Smith, R. W. R. Crevel, J. Pickup, Too clean, or not too clean: The hygiene hypothesis and home hygiene. *Clin. Exp. Allergy* **36**, 402–425 (2006).
11. C. Brooks, N. Pearce, J. Douwes, The hygiene hypothesis in allergy and asthma: An update. *Curr. Opin. Allergy Clin. Immunol.* **13**, 70–77 (2013).
12. J. Douwes, N. Pearce, D. Heederik, Does environmental endotoxin exposure prevent asthma? *Thorax* **57**, 86–90 (2002).
13. A. H. Liu, J. R. Murphy, Hygiene hypothesis: Fact or fiction? *J. Allergy Clin. Immunol.* **111**, 471–478 (2003).
14. P. S. Thorne, A. Mendy, N. Metwali, P. Salo, C. Co, R. Jaramillo, K. M. Rose, D. C. Zeldin, Endotoxin exposure: Predictors and prevalence of associated asthma outcomes in the United States. *Am. J. Respir. Crit. Care Med.* **192**, 1287–1297 (2015).

15. J. Cahenzli, Y. Köller, M. Wyss, M. B. Geuking, K. D. McCoy, Intestinal microbial diversity during early-life colonization shapes long-term IgE levels. *Cell Host Microbe* **14**, 559–570 (2013).
16. T. Herbst, A. Sichelstiel, C. Schär, K. Yadava, K. Bürki, J. Cahenzli, K. McCoy, B. J. Marsland, N. L. Harris, Dysregulation of allergic airway inflammation in the absence of microbial colonization. *Am. J. Respir. Crit. Care Med.* **184**, 198–205 (2011).
17. A. T. Stefka, T. Feehley, P. Tripathi, J. Qiu, K. McCoy, S. K. Mazmanian, M. Y. Tjota, G.-Y. Seo, S. Cao, B. R. Theriault, D. A. Antonopoulos, L. Zhou, E. B. Chang, Y.-X. Fu, C. R. Nagler, Commensal bacteria protect against food allergen sensitization. *Proc. Natl. Acad. Sci. U.S.A.* **111**, 13145–13150 (2014).
18. D. Masopust, C. P. Sivula, S. C. Jameson, Of mice, dirty mice, and men: Using mice to understand human immunology. *J. Immunol.* **199**, 383–388 (2017).
19. L. K. Beura, S. E. Hamilton, K. Bi, J. M. Schenkel, O. A. Odumade, K. A. Casey, E. A. Thompson, K. A. Fraser, P. C. Rosato, A. Filali-Mouhim, R. P. Sekaly, M. K. Jenkins, V. Vezys, W. N. Haining, S. C. Jameson, D. Masopust, Normalizing the environment recapitulates adult human immune traits in laboratory mice. *Nature* **532**, 512–516 (2016).
20. J.-D. Lin, J. C. Devlin, F. Yeung, C. McCauley, J. M. Leung, Y.-H. Chen, A. Cronkite, C. Hansen, C. Drake-Dunn, K. V. Ruggles, K. Cadwell, A. L. Graham, P. Loke, Rewilding Nod2 and Atg16l1 mutant mice uncovers genetic and environmental contributions to microbial responses and immune cell composition. *Cell Host Microbe* **27**, 830–840.e4 (2020).
21. S. P. Rosshart, J. Herz, B. G. Vassallo, A. Hunter, M. K. Wall, J. H. Badger, J. A. McCulloch, D. G. Anastasakis, A. A. Sarshad, I. Leonardi, N. Collins, J. A. Blatter, S.-J. Han, S. Tamoutounour, S. Potapova, M. B. Foster St Claire, W. Yuan, S. K. Sen, M. S. Dreier, B. Hild, M. Hafner, D. Wang, I. D. Iliev, Y. Belkaid, G. Trinchieri, B. Rehermann, Laboratory mice born to wild mice have natural microbiota and model human immune responses. *Science* **365**, eaaw4361 (2019).
22. S. P. Rosshart, B. G. Vassallo, D. Angeletti, D. S. Hutchinson, A. P. Morgan, K. Takeda, H. D. Hickman, J. A. McCulloch, J. H. Badger, N. J. Ajami, G. Trinchieri, F. Pardo-Manuel de Villena, J. W. Yewdell, B. Rehermann, Wild mouse gut microbiota promotes host fitness and improves disease resistance. *Cell* **171**, 1015–1028.e13 (2017).
23. F. Yeung, Y.-H. Chen, J.-D. Lin, J. M. Leung, C. McCauley, J. C. Devlin, C. Hansen, A. Cronkite, Z. Stephens, C. Drake-Dunn, Y. Fulmer, B. Shopsin, K. V. Ruggles, J. L. Round, P. Loke, A. L. Graham, K. Cadwell, Altered immunity of laboratory mice in the natural environment is associated with fungal colonization. *Cell Host Microbe* **27**, 809–822.e6 (2020).
24. C. Haluszczak, A. D. Akue, S. E. Hamilton, L. D. S. Johnson, L. Pujanauski, L. Teodorovic, S. C. Jameson, R. M. Kedl, The antigen-specific $CD8^+$ T cell repertoire in unimmunized mice includes memory phenotype cells bearing markers of homeostatic expansion. *J. Exp. Med.* **206**, 435–448 (2009).
25. M. Kechagia, D. Basoulis, S. Konstantopoulou, D. Dimitriadi, K. Gyftopoulou, N. Skarmoutsou, E. M. Fakiri, Health benefits of probiotics: A review. *ISRN Nutr.* **2013**, 481651 (2013).
26. Y. M. Sjögren, M. C. Jenmalm, M. F. Böttcher, B. Björkstén, E. Sverremark-Ekström, Altered early infant gut microbiota in children developing allergy up to 5 years of age. *Clin. Exp. Allergy* **39**, 518–526 (2009).
27. B. N. Lambrecht, H. Hammad, The immunology of asthma. *Nat. Immunol.* **16**, 45–56 (2015).
28. Y. Wang, M. A. Su, Y. Y. Wan, An essential role of the transcription factor GATA-3 for the function of regulatory T cells. *Immunity* **35**, 337–348 (2011).
29. E. A. Wohlfert, J. R. Grainger, N. Bouladoux, J. E. Konkel, G. Oldenhove, C. H. Ribeiro, J. A. Hall, R. Yagi, S. Naik, R. Bhairavabhotla, W. E. Paul, R. Bosselut, G. Wei, K. Zhao, M. Oukka, J. Zhu, Y. Belkaid, GATA3 controls $Foxp3^+$ regulatory T cell fate during inflammation in mice. *J. Clin. Invest.* **121**, 4503–4515 (2011).
30. D. Artis, H. Spits, The biology of innate lymphoid cells. *Nature* **517**, 293–301 (2015).
31. A. B. Molofsky, J. C. Nussbaum, H.-E. Liang, S. J. Van Dyken, L. E. Cheng, A. Mohapatra, A. Chawla, R. M. Locksley, Innate lymphoid type 2 cells sustain visceral adipose tissue eosinophils and alternatively activated macrophages. *J. Exp. Med.* **210**, 535–549 (2013).
32. I. M. de Kleer, M. Kool, M. J. W. de Bruijn, M. Willart, J. van Moorleghem, M. J. Schuijs, M. Plantinga, R. Beyaert, E. Hams, P. G. Fallon, H. Hammad, R. W. Hendriks, B. N. Lambrecht, Perinatal activation of the interleukin-33 pathway promotes type 2 immunity in the developing lung. *Immunity* **45**, 1285–1298 (2016).
33. R. M. Green, A. Custovic, G. Sanderson, J. Hunter, S. L. Johnston, A. Woodcock, Synergism between allergens and viruses and risk of hospital admission with asthma: Case-control study. *BMJ* **324**, 763 (2002).
34. C. S. Murray, G. Poletti, T. Kebadze, J. Morris, A. Woodcock, S. L. Johnston, A. Custovic, Study of modifiable risk factors for asthma exacerbations: Virus infection and allergen exposure increase the risk of asthma hospital admissions in children. *Thorax* **61**, 376–382 (2006).
35. R. Sporik, S. T. Holgate, T. A. E. Platts-Mills, J. J. Cogswell, Exposure to house-dust mite allergen (*Der p* I) and the development of asthma in childhood: A prospective study. *N. Engl. J. Med.* **323**, 502–507 (1990).
36. C. A. Tibbitt, J. M. Stark, L. Martens, J. Ma, J. E. Mold, K. Deswarte, G. Oliynyk, X. Feng, B. N. Lambrecht, P. De Bleser, S. Nylén, H. Hammad, M. Arsenian Henriksson, Y. Saeys, J. M. Coquet, Single-cell RNA sequencing of the T helper cell response to house dust mites defines a distinct gene expression signature in airway T_H2 Cells. *Immunity* **51**, 169–184.e5 (2019).
37. D. Cipolletta, M. Feuerer, A. Li, N. Kamei, J. Lee, S. E. Shoelson, C. Benoist, D. Mathis, PPAR-γ is a major driver of the accumulation and phenotype of adipose tissue T_{reg} cells. *Nature* **486**, 549–553 (2012).
38. L. D. Faustino, J. W. Griffith, R. A. Rahimi, K. Nepal, D. L. Hamilos, J. L. Cho, B. D. Medoff, J. J. Moon, D. A. A. Vignali, A. D. Luster, Interleukin-33 activates regulatory T cells to suppress innate γδ T cell responses in the lung. *Nat. Immunol.* **21**, 1371–1383 (2020).
39. W. Kuswanto, D. Burzyn, M. Panduro, K. K. Wang, Y. C. Jang, A. J. Wagers, C. Benoist, D. Mathis, Poor repair of skeletal muscle in aging mice reflects a defect in local, interleukin-33-dependent accumulation of regulatory T cells. *Immunity* **44**, 355–367 (2016).
40. C. Schiering, T. Krausgruber, A. Chomka, A. Fröhlich, K. Adelmann, E. A. Wohlfert, J. Pott, T. Griseri, J. Bollrath, A. N. Hegazy, O. J. Harrison, B. M. J. Owens, M. Löhning, Y. Belkaid, P. G. Fallon, F. Powrie, The alarmin IL-33 promotes regulatory T-cell function in the intestine. *Nature* **513**, 564–568 (2014).
41. K. J. Filbey, M. Camberis, J. Chandler, R. Turner, A. J. Kettle, R. M. Eichenberger, P. Giacomin, G. Le Gros, Intestinal helminth infection promotes IL-5- and CD4+ T cell-dependent immunity in the lung against migrating parasites. *Mucosal Immunol.* **12**, 352–362 (2019).
42. L. Guo, Y. Huang, X. Chen, J. Hu-Li, J. F. Urban Jr., W. E. Paul, Innate immunological function of T_H2 cells in vivo. *Nat. Immunol.* **16**, 1051–1059 (2015).
43. C. M. Minutti, S. Drube, N. Blair, C. Schwartz, J. C. McCrae, A. N. McKenzie, T. Kamradt, M. Mokry, P. J. Coffer, M. Sibilia, A. J. Sijts, P. G. Fallon, R. M. Maizels, D. M. Zaiss, Epidermal growth factor receptor expression licenses type-2 helper T cells to function in a T cell receptor-independent fashion. *Immunity* **47**, 710–722.e6 (2017).
44. Y. Fu, J. Wang, B. Zhou, A. Pajulas, H. Gao, B. Ramdas, B. Koh, B. J. Ulrich, S. Yang, R. Kapur, J.-C. Renauld, S. Paczesny, Y. Liu, R. M. Tighe, P. Licona-Limón, R. A. Flavell, S. Takatsuka, D. Kitamura, R. S. Tepper, J. Sun, M. H. Kaplan, An IL-9–pulmonary macrophage axis defines the allergic lung inflammatory environment. *Sci. Immunol.* **7**, eabi9768 (2022).
45. V. Vezys, A. Yates, K. A. Casey, G. Lanier, R. Ahmed, R. Antia, D. Masopust, Memory CD8 T-cell compartment grows in size with immunological experience. *Nature* **457**, 196–199 (2009).
46. S. Wijeyesinghe, L. K. Beura, M. J. Pierson, J. M. Stolley, O. A. Adam, R. Ruscher, E. M. Steinert, P. C. Rosato, V. Vezys, D. Masopust, Expansible residence decentralizes immune homeostasis. *Nature* **592**, 457–462 (2021).
47. K. E. Block, K. Iijima, M. J. Pierson, D. A. Walsh, R. Tei, T. A. Kucaba, J. Xu, M. H. Khan, C. Staley, T. S. Griffith, H. J. McSorley, H. Kita, S. C. Jameson, Physiological microbial exposure transiently inhibits mouse lung ILC2 responses to allergens. *Nat. Immunol.* **23**, 1703–1713 (2022).
48. H. E. Jakobsson, T. R. Abrahamsson, M. C. Jenmalm, K. Harris, C. Quince, C. Jernberg, B. Björkstén, L. Engstrand, A. F. Andersson, Decreased gut microbiota diversity, delayed Bacteroidetes colonisation and reduced T_H1 responses in infants delivered by caesarean section. *Gut* **63**, 559–566 (2014).
49. D. P. Strachan, Hay fever, hygiene, and household size. *BMJ* **299**, 1259–1260 (1989).
50. T. R. Abrahamsson, H. E. Jakobsson, A. F. Andersson, B. Björkstén, L. Engstrand, M. C. Jenmalm, Low diversity of the gut microbiota in infants with atopic eczema. *J. Allergy Clin. Immunol.* **129**, 434–440 (2012).
51. B. Björkstén, E. Sepp, K. Julge, T. Voor, M. Mikelsaar, Allergy development and the intestinal microflora during the first year of life. *J. Allergy Clin. Immunol.* **108**, 516–520 (2001).
52. G. den Besten, K. van Eunen, A. K. Groen, K. Venema, D.-J. Reijngoud, B. M. Bakker, The role of short-chain fatty acids in the interplay between diet, gut microbiota, and host energy metabolism. *J. Lipid Res.* **54**, 2325–2340 (2013).
53. K. M. Maslowski, A. T. Vieira, A. Ng, J. Kranich, F. Sierro, D. Yu, H. C. Schilter, M. S. Rolph, F. Mackay, D. Artis, R. J. Xavier, M. M. Teixeira, C. R. Mackay, Regulation of inflammatory responses by gut microbiota and chemoattractant receptor GPR43. *Nature* **461**, 1282–1286 (2009).
54. N. Arpaia, C. Campbell, X. Fan, S. Dikiy, J. van der Veeken, P. deRoos, H. Liu, J. R. Cross, K. Pfeffer, P. J. Coffer, A. Y. Rudensky, Metabolites produced by commensal bacteria promote peripheral regulatory T-cell generation. *Nature* **504**, 451–455 (2013).
55. A. Trompette, E. S. Gollwitzer, K. Yadava, A. K. Sichelstiel, N. Sprenger, C. Ngom-Bru, C. Blanchard, T. Junt, L. P. Nicod, N. L. Harris, B. J. Marsland, Gut microbiota metabolism of dietary fiber influences allergic airway disease and hematopoiesis. *Nat. Med.* **20**, 159–166 (2014).
56. J. R. Grainger, K. A. Smith, J. P. Hewitson, H. J. McSorley, Y. Harcus, K. J. Filbey, C. A. M. Finney, E. J. D. Greenwood, D. P. Knox, M. S. Wilson, Y. Belkaid, A. Y. Rudensky, R. M. Maizels, Helminth secretions induce de novo T cell Foxp3 expression and regulatory function through the TGF-β pathway. *J. Exp. Med.* **207**, 2331–2341 (2010).

57. C. M. Lloyd, S. Saglani, Early-life respiratory infections and developmental immunity determine lifelong lung health. *Nat. Immunol.* **24**, 1234–1243 (2023).
58. M. M. Zaiss, A. Rapin, L. Lebon, L. K. Dubey, I. Mosconi, K. Sarter, A. Piersigilli, L. Menin, A. W. Walker, J. Rougemont, O. Paerewijck, P. Geldhof, K. D. McCoy, A. J. Macpherson, J. Croese, P. R. Giacomin, A. Loukas, T. Junt, B. J. Marsland, N. L. Harris, The intestinal microbiota contributes to the ability of helminths to modulate allergic inflammation. *Immunity* **43**, 998–1010 (2015).
59. T. Haahtela, A biodiversity hypothesis. *Allergy* **74**, 1445–1456 (2019).
60. J. M. Norman, S. A. Handley, H. W. Virgin, Kingdom-agnostic metagenomics and the importance of complete characterization of enteric microbial communities. *Gastroenterology* **146**, 1459–1469 (2014).
61. J. K. Pfeiffer, H. W. Virgin, Transkingdom control of viral infection and immunity in the mammalian intestine. *Science* **351**, aad5872 (2016).
62. T. S. Stappenbeck, H. W. Virgin, Accounting for reciprocal host–microbiome interactions in experimental science. *Nature* **534**, 191–199 (2016).
63. A. Chudnovskiy, A. Mortha, V. Kana, A. Kennard, J. D. Ramirez, A. Rahman, R. Remark, I. Mogno, R. Ng, S. Gnjatic, E. D. Amir, A. Solovyov, B. Greenbaum, J. Clemente, J. Faith, Y. Belkaid, M. E. Grigg, M. Merad, Host-protozoan interactions protect from mucosal infections through activation of the inflammasome. *Cell* **167**, 444–456.e14 (2016).
64. M. R. Howitt, S. Lavoie, M. Michaud, A. M. Blum, S. V. Tran, J. V. Weinstock, C. A. Gallini, K. Redding, R. F. Margolskee, L. C. Osborne, D. Artis, W. S. Garrett, Tuft cells, taste-chemosensory cells, orchestrate parasite type 2 immunity in the gut. *Science* **351**, 1329–1333 (2016).
65. A. L. Ackerman, D. M. Underhill, The mycobiome of the human urinary tract: Potential roles for fungi in urology. *Ann. Transl. Med.* **5**, 31 (2017).
66. E. S. Lim, D. Wang, L. R. Holtz, The bacterial microbiome and virome milestones of infant development. *Trends Microbiol.* **24**, 801–810 (2016).
67. S. Runge, S. P. Rosshart, The mammalian metaorganism: A holistic view on how microbes of all kingdoms and niches shape local and systemic immunity. *Front. Immunol.* **12**, 702378 (2021).
68. J. Friesen, C. Bergmann, R. Neuber, J. Fuhrmann, T. Wenzel, A. Durst, M. Müller, R. Ignatius, Detection of *Enterobius vermicularis* in greater Berlin, 2007–2017: Seasonality and increased frequency of detection. *Eur. J. Clin. Microbiol. Infect. Dis.* **38**, 719–723 (2019).
69. S. Wendt, H. Trawinski, S. Schubert, A. C. Rodloff, J. Mössner, C. Lübbert, The diagnosis and treatment of pinworm infection. *Dtsch. Arztebl. Int.* **116**, 213–219 (2019).
70. S. S. Agersborg, K. M. Garza, K. S. K. Tung, Intestinal parasitism terminates self tolerance and enhances neonatal induction of autoimmune disease and memory. *Eur. J. Immunol.* **31**, 851–859 (2001).
71. C. Michels, P. Goyal, N. Nieuwenhuizen, F. Brombacher, Infection with *Syphacia obvelata* (pinworm) induces protective T_H2 immune responses and influences ovalbumin-induced allergic reactions. *Infect. Immun.* **74**, 5926–5932 (2006).
72. R. Crameri, M. Garbani, C. Rhyner, C. Huitema, Fungi: The neglected allergenic sources. *Allergy* **69**, 176–185 (2014).
73. T. A. E. Platts-Mills, Asthma severity and prevalence: An ongoing interaction between exposure, hygiene, and lifestyle. *PLOS Med.* **2**, e34 (2005).
74. T. A. E. Platts-Mills, E. Erwin, P. Heymann, J. Woodfolk, Is the hygiene hypothesis still a viable explanation for the increased prevalence of asthma? *Allergy* **60**, 25–31 (2005).
75. M. E. Rothenberg, The climate change hypothesis for the allergy epidemic. *J. Allergy Clin. Immunol.* **149**, 1522–1524 (2022).
76. S.-N. Yang, C.-C. Hsieh, H.-F. Kuo, M.-S. Lee, M.-Y. Huang, C.-H. Kuo, C.-H. Hung, The effects of environmental toxins on allergic inflammation. *Allergy Asthma Immunol. Res.* **6**, 478–484 (2014).
77. J. G. Caporaso, J. Kuczynski, J. Stombaugh, K. Bittinger, F. D. Bushman, E. K. Costello, N. Fierer, A. G. Peña, J. K. Goodrich, J. I. Gordon, G. A. Huttley, S. T. Kelley, D. Knights, J. E. Koenig, R. E. Ley, C. A. Lozupone, D. McDonald, B. D. Muegge, M. Pirrung, J. Reeder, J. R. Sevinsky, P. J. Turnbaugh, W. A. Walters, J. Widmann, T. Yatsunenko, J. Zaneveld, R. Knight, QIIME allows analysis of high-throughput community sequencing data. *Nat. Methods* **7**, 335–336 (2010).
78. W. G. Weisburg, S. M. Barns, D. A. Pelletier, D. J. Lane, 16*S* ribosomal DNA amplification for phylogenetic study. *J. Bacteriol.* **173**, 697–703 (1991).
79. R. C. Edgar, Search and clustering orders of magnitude faster than BLAST. *Bioinformatics* **26**, 2460–2461 (2010).
80. Q. Wang, G. M. Garrity, J. M. Tiedje, J. R. Cole, Naïve bayesian classifier for rapid assignment of rRNA sequences into the new bacterial taxonomy. *Appl. Environ. Microbiol.* **73**, 5261–5267 (2007).
81. M. N. Price, P. S. Dehal, A. P. Arkin, FastTree 2–Approximately maximum-likelihood trees for large alignments. *PLOS ONE* **5**, e9490 (2010).
82. P. J. McMurdie, S. Holmes, phyloseq: An R package for reproducible interactive analysis and graphics of microbiome census data. *PLOS ONE* **8**, e61217 (2013).
83. B. D. Hondowicz, D. An, J. M. Schenkel, K. S. Kim, H. R. Steach, A. T. Krishnamurty, G. J. Keitany, E. N. Garza, K. A. Fraser, J. J. Moon, W. A. Altemeier, D. Masopust, M. Pepper, Interleukin-2-dependent allergen-specific tissue-resident memory cells drive asthma. *Immunity* **44**, 155–166 (2016).
84. R. W. Nelson, D. Beisang, N. J. Tubo, T. Dileepan, D. L. Wiesner, K. Nielsen, M. Wüthrich, B. S. Klein, D. I. Kotov, J. A. Spanier, B. T. Fife, J. J. Moon, M. K. Jenkins, T cell receptor cross-reactivity between similar foreign and self peptides influences naive cell population size and autoimmunity. *Immunity* **42**, 95–107 (2015).

Acknowledgments: We would like to thank the staff at KM-F animal facility for facilitating the transport and animal husbandry of wildling mice. Pathological analysis of some lung tissue was performed at the Morphological Phenotype Analysis Facility at Karolinska Institutet. We thank the NIH Tetramer Core Facility for tetramers to detect HDM-specific CD4, NKT, and MAIT T cells. We thank L. Westerberg, P. Dosenovic, G. K. Hedestam, T. Kreslavskiy, E. Winkler, M. A. P. Garasa, V. Krmeská, and A. L. Clavero for reagents and technical assistance. J.M.C. also thanks his mother Roselyn for traveling to Copenhagen and looking after her three grandchildren, which allowed us to finalize this manuscript. **Funding:** J.M.C. and J.D. were supported by the Swedish Research Council (2018-02536 and 2021-01683, respectively) and Swedish Cancer foundation (CAN2017/715 and 20 0261 F). S.N. and C.H.C. were supported by KI intramural funds. S.P.R. was supported by the DFG Emmy Noether-Programm RO 6247/1-1 (project ID 446316360), the DFG SFB1160 IMPATH (project ID 256073931), and the TRR 359 PILOT (project ID 491676693). J.M. was supported by a Chinese Scholarship Council fellowship, and E.U. was supported by the Wenner Gren foundation. T.S. was funded by the Deutsche Forschungsgemeinschaft (DFG; German Research Foundation) under Germany's Excellence Strategy–EXC 2155 (project number 390874280). **Author contributions:** Conceptualization: J.M.C., S.P.R., and S.N. Methodology: J.M., S.P.R., S.N., S.V., H.-J.H., E.U., S.R., R.B., L.B., M.A., J.D., S.v.Z., A.M.G., A.A.B., and T.R.L. Investigation: J.M., E.U., S.R., C.H.C., J.M.S., M.L., L.M., I.M.G., L.C., J.M.C., S.N., S.v.Z., J.A., A.B., S.M.H., L.O., T.S., and A.M.G. Data curation and visualization: J.M., E.U., S.R., J.M.S., J.M.C., and S.P.R. Funding acquisition: J.M.C., S.N., S.P.R., and J.D. Supervision: J.M.C., S.N., S.P.R., and J.D. Writing—original draft: J.M. and J.M.C. Writing—review and editing: J.M.C., S.P.R., and S.N. **Competing interests:** S.P.R. declares that he has no competing interests and discloses that Taconic Biosciences licensed WildR mice with natural gut microbiota from NIDDK. L.B. is Chief Scientific Officer and board member from JJP Biologics. All other authors declare that they have no competing interests. **Data and materials availability:** C57BL/6NTac mice with natural wild mouse microbiota and pathogens at all body sites are available from S.P.R. under a material transfer agreement with the Department of Microbiome Research, University Hospital Erlangen, Friedrich-Alexander-Universität Erlangen-Nürnberg (FAU), Germany. Sequencing datasets have been deposited to NCBI as a Bioproject under accession number PRJEB65584 (https://ncbi.nlm.nih.gov/). All data needed to evaluate the conclusions in the paper are present in the paper or the Supplementary Materials.

Submitted 11 November 2022
Accepted 30 August 2023
Published 29 September 2023
10.1126/sciimmunol.adf7702